

Barrier-crossing and energy relaxation dynamics of non-Markovian inertial systems connected via analytical Green-Fokker-Planck approach

Roland R. Netz

Fachbereich Physik, Freie Universität Berlin, 144195 Berlin, Germany

(Dated: January 16, 2026)

From numerical simulations it is known that the barrier-crossing time of a non-Markovian one-dimensional reaction coordinate with a single exponentially decaying memory function exhibits a memory-turnover: for intermediate values of the memory decay time the barrier-crossing time is reduced compared to the Markovian limit and for long memory times increases quadratically with the memory time when keeping the total integrated friction and the mass constant. The intermediate memory acceleration regime is accurately predicted by Grote-Hynes theory, for the asymptotic long-memory slow-down behavior no systematic analytically tractable theory is available. Starting from the Green function for a general inertial (i.e. finite-mass) non-Markovian Gaussian reaction coordinate in a harmonic well, we derive by an exact mapping a generalized Fokker-Planck equation with a time-dependent effective diffusion constant. To first order in a systematic cumulant expansion we derive an analytical Arrhenius expression for the barrier-crossing time with the pre-exponential factor given by the energy relaxation time, which can be used to robustly predict barrier-crossing times from simulation or experimental trajectory data of general non-Markovian inertial systems without the need to extract memory functions. For a single exponential memory kernel we give a closed-form expression for the barrier-crossing time, which reproduces the Kramers turnover between the high-friction and high-mass limits as well as the memory turnover from the intermediate memory acceleration to the asymptotic long-memory slow-down regime. We also show that non-Markovian systems are singular in the zero-mass limit, which suggests that the long-memory barrier-crossing slow-down reflects the interplay between mass and memory effects. Thus, physically sound models for non-Markovian systems have to include a finite mass.

I. INTRODUCTION

Rare events, that means chemical reactions, conformational molecular transformation or nucleation in metastable bulk systems, involve in their time-limiting step the crossing of a free-energetic barrier when described in terms of low- or one-dimensional reaction coordinates [1–6]. The theoretical description of such barrier-crossing phenomena has a long history in physics and chemistry [7]. Arrhenius showed that for a system in contact with a heat bath, the typical barrier-crossing time scales as $\tau_0 e^{\beta U_0}$, where $\beta = 1/(k_B T)$ is the inverse thermal energy, U_0 is the height of the barrier in the free-energy landscape, and τ_0 is a prefactor [8]. That prefactor depends not only on the free-energy profile, as in transition-state theory [9, 10], but also on the dissipative coupling to the environment [1–6, 11–13]. Kramers calculated τ_0 in the Markovian limit, where environmental dissipation is described by a time-independent friction coefficient γ , implying infinitely fast environmental relaxation dynamics [1]. He derived explicit formulas for τ_0 in the high-friction limit, where inertial effects due to the effective mass of the reaction coordinate can be neglected, as well as in the low-friction limit, where inertial relaxation effects become dominant. The crossover between these asymptotic limits, known as the Kramers turnover regime, was considered in many works [14–16].

However, physical environments do not relax instantaneously. The influence of finite environmental relaxation times on reaction coordinate dynamics was explored by Zwanzig [17] and Mori [18], who used pro-

jection techniques to show that the dynamics of a low-dimensional observable defined for a general many-body system is described by the generalized Langevin equation (GLE). The GLE is an integro-differential equation that generalizes the Newtonian equation of motion by explicitly accounting for the coupling of the observable to its responsive environment in terms of a non-Markovian (i.e. time-dependent) friction memory kernel $\Gamma(t)$ and a time-dependent force. Thus, the GLE correctly accounts for the loss of information when projecting the high-dimensional phase-space dynamics onto the low-dimensional observable dynamics and constitutes an exact coarse-graining method. An alternative strategy to eliminate or reduce non-Markovian effects is to use suitable multidimensional reaction coordinates that explicitly account for solvent degrees of freedom, which basically corresponds to the Markovian-embedding treatment of a GLE with multi-exponential memory kernel [19]. Several methods to extract all GLE parameters from time-series data exist [20–30] and using such methods the GLE has been applied to bond-length vibrations [31–33], dihedral rotations [3, 25, 34, 35], chemical reactions in solvents [36–39], protein folding [40–45] and also more complex systems, such as the motion of living organisms as well as genetic, financial and meteorological data [46–53].

Grote and Hynes (GH) derived a self-consistent equation for barrier-crossing rates in systems with short memory times in the medium- to high-friction regime [54], which was subsequently successfully applied to different barrier-crossing phenomena in liquids [55, 56]. Polak, Grabert, and Hänggi subsequently constructed a

theory also applicable for long memory times [57, 58], which however does not allow to analytically extract the asymptotic dependence of barrier-crossing times on the memory time. Many barrier-crossing rate theories represent the free-energy landscape as an inverted parabola and thereby neglect relaxation in a free-energy minimum prior to a transition. However, as we show in this paper, this relaxation is important particularly for long memory times, therefore the barrier free-energy landscape is more realistically modeled as a single-well or double-well potential, relevant, for example, to chemical reactions and protein folding [6, 7, 59–62]. In fact, from numerical simulations it is known that the barrier-crossing time of a non-Markovian one-dimensional reaction coordinate with a single exponentially decaying memory function exhibits a non-monotonic dependence on the memory time [63]: keeping the friction (i.e. the integral over the memory function) constant, for intermediate values of the memory time the barrier-crossing time is reduced compared to the Markovian limit but for long memory times increases quadratically with the memory time [64–66]. The intermediate memory acceleration regime is accurately predicted by Grote-Hynes theory, for the asymptotic long-memory slow-down behavior no systematic analytically tractable theory is available, a gap that is filled in this paper.

Starting from the Green function for a general inertial non-Markovian Gaussian reaction coordinate in a harmonic well given in Sec. II A, we derive in Sec. II B by an exact mapping a generalized Fokker-Planck equation with a time-dependent effective diffusion constant that accounts for non-Markovian and inertial effects. Using the propagator of the generalized Fokker-Planck operator, absorbing and reflecting boundary conditions are introduced in Sec. II C. To first order in a cumulant expansion of the time-dependent diffusion constant, we derive in Sec. II D an analytical expression for the pre-exponential factor of the Arrhenius prediction for the barrier-crossing time that involves the integral over the potential-energy correlation function. This expression can be straightforwardly applied to simulation and experimental trajectory data without the need to extract memory functions, as is necessary for standard non-Markovian reaction rate theories. The influence of different potential shapes on the mean-first passage time is treated in Sec. II E. In Sec. II F we derive a closed-form expression for the barrier-crossing time for a single exponential memory kernel, which reproduces the Kramers turnover between the Markovian high-friction and high-mass limits as well as the memory turnover from the intermediate memory acceleration, where agreement with Grote-Hynes theory is obtained, to the asymptotic long-memory slow-down regime. In Sec. II G we demonstrate that non-Markovian systems are singular in the mass-less limit. In Sec. II H we show that the Langevin equation, when properly derived from the GLE in the memory-less limit, preserves time reversibility, as opposed to usual formulations of the Langevin equation in literature. Section III summarizes

our results in a condensed set of equations and compares our predictions of barrier-crossing times with previously published simulations results.

II. RESULTS

A. Non-Markovian Green function

We consider the dynamics of a general non-Markovian stochastic process in a harmonic potential well. Neglecting possible non-linear friction effects, the process is Gaussian and the two-point positional joint distribution for the position to be x at time t and x_0 at time zero in all generality is given by

$$\mathcal{P}(x, t; x_0) = \exp(-a(t)x^2/2 - b(t)xx_0 - c(t)x_0^2/2) \mathcal{N}^{-1}, \quad (1)$$

where \mathcal{N} is the normalization constant and $a(t)$, $b(t)$, $c(t)$ are unknown time-dependent functions. These four unknowns are determined by the following four conditions:

i) For a stationary process (assumed in this work) the joint distribution is symmetric, i.e.,

$$\mathcal{P}(x, t; x_0) = \mathcal{P}(x_0, t; x), \quad (2)$$

ii) the joint distribution is normalized,

$$\int_{-\infty}^{\infty} dx \int_{-\infty}^{\infty} dx_0 \mathcal{P}(x, t; x_0) = 1, \quad (3)$$

iii) the covariance of the distribution defines the two-point correlation function

$$\int_{-\infty}^{\infty} dx \int_{-\infty}^{\infty} dx_0 xx_0 \mathcal{P}(x, t; x_0) \equiv \langle xx_0 \rangle \equiv C(t), \quad (4)$$

and iv) the variance of the distribution is denoted as C_0

$$\int_{-\infty}^{\infty} dx \int_{-\infty}^{\infty} dx_0 x^2 \mathcal{P}(x, t; x_0) = \langle x^2 \rangle = C(0) \equiv C_0 \quad (5)$$

(note that due to symmetry we have $\langle x^2 \rangle = \langle x_0^2 \rangle$). With these four relations, the joint distribution can be written in terms of the correlation function $C(t)$ as

$$\mathcal{P}(x, t; x_0) = \frac{\exp\left(-\frac{(x-\bar{C}(t)x_0)^2}{2C_0(1-\bar{C}^2(t))} - \frac{x_0^2}{2C_0}\right)}{2\pi C_0 (1 - \bar{C}^2(t))}, \quad (6)$$

where we introduced the normalized two-point correlation function as

$$\bar{C}(t) = C(t)/C_0, \quad (7)$$

see Appendix A for details. Using the single-point distribution function, which is obtained via marginalization of Eq.(6) as

$$\mathcal{P}(x) \equiv \int_{-\infty}^{\infty} dx_0 \mathcal{P}(x, t; x_0) = \frac{\exp\left(-\frac{x^2}{2C_0}\right)}{[2\pi/C_0]^{1/2}}, \quad (8)$$

the conditional two-point distribution is obtained as

$$\mathcal{P}(x, t|x_0) = \frac{\mathcal{P}(x, t; x_0)}{\mathcal{P}(x_0)} = \frac{\exp\left(-\frac{(x-\bar{C}(t)x_0)^2}{2C_0(1-\bar{C}^2(t))}\right)}{[2\pi C_0(1-\bar{C}^2(t))]^{1/2}}. \quad (9)$$

In fact, the expression Eq.(9) has been recently derived from the generalized Langevin equation using stochastic path-integral formalism [67], which underscores the exactness of the current symmetry-based derivation. Since the conditional two-point distribution in Eq.(9) corresponds to the distribution generated by the non-Markovian process with the initial probability distribution $\mathcal{P}(x, t=0|x_0) = \delta(x - x_0)$, it constitutes the Green function of the process.

B. From the non-Markovian Green function to the generalized Fokker-Planck equation

By taking a partial derivative of the Green function Eq.(9) with respect to time, we obtain an expression that can be brought into the form of a partial differential equation

$$\frac{\partial \mathcal{P}(x, t|x_0)}{\partial t} = -\frac{C_0 \bar{C}'(t)}{\bar{C}(t)} \left[\frac{\partial}{\partial x} \frac{x}{C_0} + \frac{\partial^2}{\partial x^2} \right] \mathcal{P}(x, t|x_0), \quad (10)$$

where $\bar{C}'(t)$ denotes the derivate of $\bar{C}(t)$, see Appendix B for intermediate steps of the derivation. The Green function of the Gaussian process in Eq.(9) is valid for a harmonic potential of the form

$$U(x) = Kx^2/2, \quad (11)$$

for which the variance follows for a canonical system at temperature T from the equipartition theorem as $C_0 = k_B T/K$, where k_B is the Boltzmann constant. With this we can rewrite Eq. (11) in the form

$$\begin{aligned} \frac{\partial \mathcal{P}(x, t|x_0)}{\partial t} &= D(t) \left[\frac{\partial}{\partial x} \beta U'(x) + \frac{\partial^2}{\partial x^2} \right] \mathcal{P}(x, t|x_0) \\ &= D(t) \frac{\partial}{\partial x} e^{-\beta U(x)} \frac{\partial}{\partial x} e^{\beta U(x)} \mathcal{P}(x, t|x_0), \end{aligned} \quad (12)$$

where we used $\beta = 1/(k_B T)$ and introduced the time-dependent diffusivity

$$D(t) = -\frac{C_0 \bar{C}'(t)}{\bar{C}(t)} = -\frac{C_0 C'(t)}{C(t)}. \quad (13)$$

By writing the probability distribution as a convolution of the Green function $\mathcal{P}(x, t|x_0)$ with the initial distribution $\mathcal{P}_0(x_0)$ as

$$\mathcal{P}(x, t) = \int_{-\infty}^{\infty} dx_0 \mathcal{P}_0(x_0) \mathcal{P}(x, t|x_0), \quad (14)$$

we obtain from Eq. (12) an equation for the distribution function

$$\frac{\partial \mathcal{P}(x, t)}{\partial t} = D(t) \frac{\partial}{\partial x} e^{-\beta U(x)} \frac{\partial}{\partial x} e^{\beta U(x)} \mathcal{P}(x, t) \quad (15)$$

with the initial condition $\mathcal{P}(x, 0) = \mathcal{P}_0(x)$. This equation is identical to the standard Fokker-Planck equation for an overdamped Markovian reaction coordinate [68] except that the diffusivity $D(t)$ is time-dependent. This time-dependency takes care of inertial and non-Markovian effects and therefore contains the crucial physics we are interested in.

C. Barrier-crossing times from the generalized Fokker-Planck equation

In the following we extend the method to calculate mean-first-passage times from the standard Fokker-Planck equation with a time-independent diffusivity [68] to the case of a time-dependent diffusivity. The solution of the generalized Fokker-Planck equation for the Green function Eq. (12) can be written formally as an operator exponential as

$$\mathcal{P}(x, t|x_0) = e^{T(t)\mathcal{D}(x)} \mathcal{P}(x, 0|x_0), \quad (16)$$

where we defined the diffusive Fokker-Planck propagator as

$$\mathcal{D}(x) \equiv \frac{\partial}{\partial x} e^{-\beta U(x)} \frac{\partial}{\partial x} e^{\beta U(x)} \quad (17)$$

and the running integral over the diffusivity as

$$T(t) \equiv \int_0^t ds D(s). \quad (18)$$

Note that Eq. (16), which employs operator-exponential formalism [68], is the same Green function as given in Eq. (9), but is more useful for imposing spatial boundary conditions as needed for calculating the mean-first passage time. Using that $\mathcal{P}(x, 0|x_0) = \delta(x - x_0)$, we can write the Green function in Eq. (16) in symmetric form as

$$\begin{aligned} \mathcal{P}(x, t|x_0) &= \int_{-\infty}^{\infty} d\tilde{x} \delta(\tilde{x} - x) e^{T(t)\mathcal{D}(\tilde{x})} \delta(\tilde{x} - x_0) \\ &= \int_{-\infty}^{\infty} d\tilde{x} \delta(\tilde{x} - x_0) e^{T(t)\mathcal{D}^{\dagger}(\tilde{x})} \delta(\tilde{x} - x) \\ &= e^{T(t)\mathcal{D}^{\dagger}(x_0)} \mathcal{P}(x, 0|x_0), \end{aligned} \quad (19)$$

where we defined the adjunct Fokker-Planck operator as

$$\mathcal{D}^{\dagger}(x) \equiv e^{\beta U(x)} \frac{\partial}{\partial x} e^{-\beta U(x)} \frac{\partial}{\partial x}. \quad (20)$$

From Eqs. (16) and (19) it transpires that the Green function satisfies the normal Fokker-Planck Eq. (12) as

well as the adjunct (backward) Fokker-Planck equation, i.e.

$$\begin{aligned}\frac{\partial \mathcal{P}(x, t|x_0)}{\partial t} &= D(t)\mathcal{D}(x) \mathcal{P}(x, t|x_0) \\ &= D(t)\mathcal{D}^\dagger(x_0) \mathcal{P}(x, t|x_0).\end{aligned}\quad (21)$$

We define the survival probability in the domain between a reflecting boundary condition at x_{ref} and an absorbing boundary condition at the position $x_f > x_{\text{ref}}$ as

$$S(x_0, t) = \int_{x_{\text{ref}}}^{x_f} dx \mathcal{P}(x, t|x_0), \quad (22)$$

which has the limits $S(x_0, 0) = 1$ and $S(x_0, \infty) = 0$ for $x_{\text{ref}} < x_0 < x_f$. The first-passage (or escape) distribution follows from the time derivative of the survival probability as

$$\begin{aligned}k(x_0, t) \equiv -\frac{\partial}{\partial t} S(x_0, t) &= -\int_{x_{\text{ref}}}^{x_f} dx \frac{\partial}{\partial t} \mathcal{P}(x, t|x_0) \\ &= -\int_{x_{\text{ref}}}^{x_f} dx D(t) \mathcal{D}(x) \mathcal{P}(x, t|x_0) \\ &= -D(t) e^{-\beta U(x_f)} \frac{\partial}{\partial x_f} e^{\beta U(x_f)} \mathcal{P}(x_f, t|x_0),\end{aligned}\quad (23)$$

where we employed Eq. (21) and used in the last step that the probability flux at x_{ref} vanishes. Applying the operator expression for $k(x_0, t)$ in Eq. (23) onto the adjunct Fokker-Planck Eq. (21), we obtain

$$\frac{\partial k(x_0, t)}{\partial t} = D(t) \mathcal{D}^\dagger(x_0) k(x_0, t). \quad (24)$$

From this partial differential equation for the first-passage distribution we can recursively determine moments of the product of the first-passage distribution and the diffusivity defined as

$$k_n(x_0) \equiv \int_0^\infty dt t^n D(t) k(x_0, t) / D_0, \quad (25)$$

where D_0 is the diffusivity in a suitably defined limit, as will be discussed further below. For the first moment we obtain from Eq. (24)

$$\begin{aligned}\mathcal{D}^\dagger(x_0) k_1(x_0) &= \int_0^\infty dt t \frac{\partial}{\partial t} k(x_0, t) / D_0 \\ &= -\int_0^\infty dt k(x_0, t) / D_0 = -1/D_0,\end{aligned}\quad (26)$$

where we used that $k(x_0, \infty) = 0$ and that the time integral over $k(x_0, t)$ is normalized to unity. This equation can be inverted and yields

$$k_1(x_0) = D_0^{-1} \int_{x_0}^{x_f} dx e^{\beta U(x)} \int_{x_{\text{ref}}}^x dx' e^{-\beta U(x')}. \quad (27)$$

Note that from the definition Eq. (25) it transpires that $k_1(x_0)$ only corresponds to the mean-first passage time

τ_{mfp} , which is the average time to reach the final position x_f for the first time when starting from x_0 , if the diffusivity $D(t)$ is time-independent and given by D_0 . If, on the other hand, the diffusivity $D(t)$ is time dependent, $k_1(x_0)$ does not equal τ_{mfp} , in which case there are different ways of how to proceed. Using that the first-passage distribution for high barriers decays single-exponentially as $k(x_0, t) \simeq e^{-t/\tau_{\text{mfp}}} / \tau_{\text{mfp}}$, τ_{mfp} is determined by the equation following from combining Eq. (25) for $n = 1$ and given $D(t)$ with Eq. (27). A numerical solution of the resulting equation is possible if the two-point correlation function $C(t)$ is known reliably and the diffusivity profile $D(t)$ can via Eq. (13) be accurately calculated. In typical simulation or experimental scenarios, however, the correlation function becomes noisy in the long-time limit and thus $D(t \rightarrow \infty)$ cannot be reliably estimated. An additional problem is that $D(t)$ for inertial and non-Markovian systems typically oscillates in the long-time limit and thus the limit $D(t \rightarrow \infty)$ is not uniquely determined, as will be seen later. In the following section we will introduce a robust expansion method for $D(t)$, which allows us to replace $D(t)$ by a constant D_0 to leading order in a systematic cumulant expansion.

D. Cumulant expansion of the time-dependent diffusivity $D(t)$

The key observation is that for a single-exponential correlation function $C(t)$, the diffusivity $D(t)$ defined in Eq. (13) becomes time-independent, i.e. $D(t) = D_0$, and thus the mean-first passage time equals the first moment in Eq. (27), i.e. $\tau_{\text{mfp}} = k_1(x_0)$. This is a non-trivial observation, as the correlation function of non-Markovian and inertial systems do for specific parameter combinations indeed decay single-exponentially, as will be explicitly demonstrated below. The idea pursued in this section is to characterize deviations of $C(t)$ from a single-exponential function by a systematic cumulant expansion.

To proceed, we rewrite Eq. (13) as

$$D(t) = -\frac{C_0 \bar{C}'(t)}{\bar{C}(t)} = -\frac{C_0}{p} \frac{d\bar{C}^p(t)/dt}{\bar{C}^p(t)}, \quad (28)$$

where p is an arbitrary positive integer number that will be discussed and chosen later. We furthermore define the single-sided function

$$\phi(t) \equiv -\theta(t) \frac{d\bar{C}^p(t)}{dt}, \quad (29)$$

where $\theta(t)$ defines the Heaviside function. The Fourier transform of $\phi(t)$ can be written as a power series in frequency according to

$$\begin{aligned}\tilde{\phi}(\omega) &= \int_{-\infty}^{\infty} dt e^{-i\omega t} \phi(t) \\ &= 1 - i\omega \sum_{n=0}^{\infty} \frac{(-i\omega)^n}{n!} M_n,\end{aligned}\quad (30)$$

where we defined moments of the p -th power of the correlation function as

$$M_n = \int_0^\infty dt t^n \bar{C}^p(t). \quad (31)$$

As the only requirement, we assume all higher moments M_n to exist, which is satisfied for exponentially decaying correlation functions, which is the normal scenario. Note that by virtue of the presence of the derivative in the definition of $\phi(t)$ in Eq. (29) and the single-sidedness of $\phi(t)$, the power series in Eq. (30) starts with unity, which is crucial. In order to make the back-Fourier transform integrable, we define the inverse power series

$$\tilde{\phi}(\omega) = \left[1 + i\omega \sum_{n=0}^{\infty} \omega^n B_n \right]^{-1} \quad (32)$$

with coefficients B_n that follow uniquely from the set of moments M_m with $m \leq n$ by standard power-series inversion. To illustrate this, we write out the first two terms explicitly

$$\begin{aligned} \tilde{\phi}(\omega) &= 1 - i\omega M_0 - \omega^2 M_1 + \dots \\ &= [1 + i\omega M_0 + \omega^2 (M_1 - M_0^2) + \dots]^{-1}. \end{aligned} \quad (33)$$

It transpires that $\tilde{\phi}(\omega)$, when written as an inverse power series in ω , contains multiple poles that will lead upon back-Fourier-transforming to a sum of exponentially decaying functions. To linear order in ω we find $\tilde{\phi}(\omega) \simeq 1/(1 + i\omega M_0)$, which leads to the single exponential

$$\phi(t) \simeq \theta(t) e^{-t/M_0} / M_0. \quad (34)$$

Since for a single exponential correlation function $\bar{C}(t) = e^{-t/\tau}$ one has $M_1 = M_0^2$, one finds that in this case the second-order correction in ω in Eq. (33) vanishes (and so do all higher-order corrections). In essence, the cumulant expansion allows to write down a functional expansion in terms of deviations of the correlation function $\bar{C}(t)$ from a single-exponential form. Note that the first-order result in Eq. (34) does not reproduce the long-time asymptotic decay of $\phi(t)$ in case there are competing exponentially decaying contributions, this is particularly true for correlation functions that asymptotically oscillate, as is the case for highly inertial or highly non-Markovian systems, which will be illustrated below.

We so far have considered the numerator of Eq. (28). The denominator of Eq. (28) can for $t > 0$ be expressed in terms of the function $\phi(t)$ as

$$\bar{C}^p(t) = - \int_t^\infty ds \frac{d \bar{C}^p(s)}{ds} = \int_t^\infty ds \phi(s) \simeq e^{-t/M_0}, \quad (35)$$

where in the last step we used the first-order result from Eq. (34). By combining the results in Eqs. (34) and (35)

we obtain from Eq. (28) for the diffusivity to leading order in the cumulant expansion

$$D(t) \simeq D_0 \equiv \frac{C_0}{\tau_{\text{rel}}} = \frac{C_0}{pM_0}, \quad (36)$$

where we defined the relaxation time as $\tau_{\text{rel}} \equiv C_0/D_0$, for which we obtain to leading order in the cumulant expansion $\tau_{\text{rel}} = pM_0$. For $p = 2$, which is a natural choice as we will show below, the relaxation time follows from Eq. (31) as the integral over the squared correlation function

$$\begin{aligned} \tau_{\text{rel}} &= 2 \int_0^\infty dt \bar{C}^2(t) = \frac{2}{C_0^2} \int_0^\infty dt C^2(t) \\ &= \frac{K^2}{(k_B T)^2} \int_0^\infty dt (\langle x^2(t)x^2(0) \rangle - \langle x^2 \rangle^2), \end{aligned} \quad (37)$$

where in the last line we used Wick's theorem to show the correspondence to the potential-energy correlation function (in the following simply called the energy correlation function). Note that higher-order corrections can be calculated by carrying the cumulant expansion in Eq. (33) to higher order in ω , in which case the diffusivity $D(t)$ becomes time-dependent and the mean-first-passage time τ_{mfp} does not equal the first moment in Eq. (27), which is not pursued in this paper.

To show that $p = 2$ is a rather natural choice, we consider the average over the time-dependent diffusivity defined in Eq. (28) with a weight function $w(t)$, which we take to be given by the p -th power of the rescaled correlation function, $w(t) = \bar{C}^p(t)$, according to

$$\bar{D} = \frac{\int_0^\infty dt D(t) w(t)}{\int_0^\infty dt w(t)} = -C_0 \frac{\int_0^\infty dt \bar{C}'(t) \bar{C}^{p-1}(t)}{\int_0^\infty dt \bar{C}^p(t)} = \frac{C_0}{pM_0}. \quad (38)$$

We see that we reproduce exactly the result for D_0 in Eq. (36), which means that the leading order of the cumulant expansion corresponds to the average over $D(t)$ with a weight function proportional to $\bar{C}^p(t)$. This makes sense, since an effective time-independent diffusivity should reflect the time-dependent diffusivity in the time range that is relevant for the escape process. Since the idea of a weighting function implies a positive definite function and the correlation function $\bar{C}(t)$ can be negative even in the asymptotic long-time limit, an even exponent p makes sense. Furthermore, for $p = 2$ the relaxation time defined in Eq. (34) corresponds to the energy relaxation time, which makes also intuitive sense, as barrier-crossing involves energy relaxation. Thus, we will use $p = 2$ in all further calculations and confirm the validity of this choice by comparison with previously published mean-first passage times determined from simulations of barrier crossing dynamics in double-well potentials.

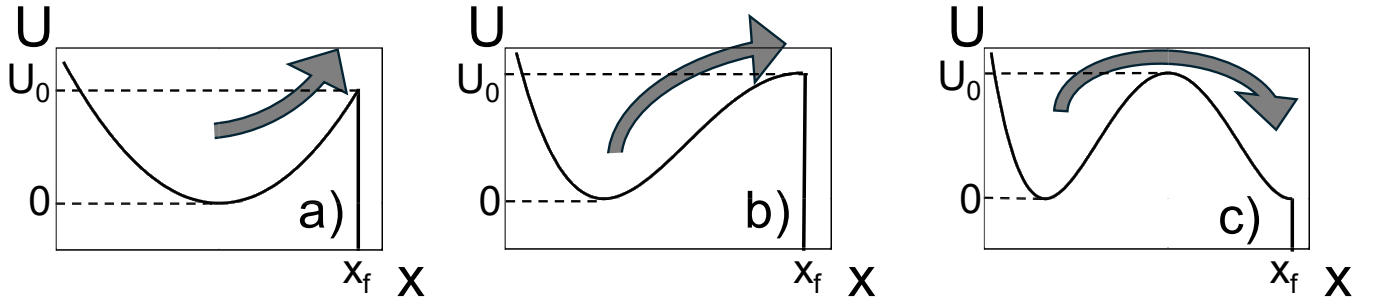


FIG. 1. Illustration of different potential shapes considered for the calculation of the mean-first passage time according to Eq. (27). The adsorbing boundary condition is indicated by an abrupt decrease of the potential. a) Harmonic potential. b) Absorbing potential is located on the top of a barrier with vanishing slope. c) Absorbing boundary condition is located to the right of the barrier.

E. Explicit predictions for different potential shapes

In the high-barrier limit the double integral in Eq. (27) can be solved by saddle-point methods [68]. In Fig. 1 the absorbing boundary condition is for a few different potentials illustrated by an abrupt decrease of the potential, indicating that a particle coming from the left that crosses the absorbing boundary condition will not be able to return back to the left. Since the Green function is calculated using Gaussian methods, our results are exact (except for the cumulant expansion used to approximate the diffusivity $D(t)$ as a constant D_0) for the harmonic potential shown in Fig. 1a). Our methods are expected to be also rather accurate for the mean-first passage time to reach the barrier top, illustrated in Fig. 1b, since the difference to a harmonic potential in a) is rather small. The difference of the mean-first passage time between crossing over the barrier to the other side of a double-well potential, as illustrated in Fig. 1c), and reaching the barrier-top, as illustrated in Fig. 1b), however, is not expected to be represented accurately by our method for strongly non-Markovian systems.

To first order in the cumulant expansion introduced in Section II D and using the saddle-point approximation, the mean-first passage time to reach the sharp-kink barrier of a harmonic potential (scenario in Fig. 1a) follows from Eq. (27) as

$$\tau_{\text{mfp}}^a = \sqrt{\frac{\pi}{\beta U_0}} \frac{e^{\beta U_0}}{D_0 \beta K} = \tau_{\text{rel}} \sqrt{\frac{\pi}{\beta U_0}} e^{\beta U_0}, \quad (39)$$

the mean-first passage time to reach the flat barrier top (scenario in Fig. 1b) reads

$$\tau_{\text{mfp}}^b = \frac{\pi e^{\beta U_0}}{D_0 \beta \sqrt{K K_{\text{bar}}}} = \pi \tau_{\text{rel}} \left(\frac{K}{K_{\text{bar}}} \right)^{1/2} e^{\beta U_0}, \quad (40)$$

and the mean-first passage time to reach over the barrier to the other side (scenario in Fig. 1c) is given by

$$\tau_{\text{mfp}}^c = \frac{2\pi e^{\beta U_0}}{D_0 \beta \sqrt{K K_{\text{bar}}}} = 2\pi \tau_{\text{rel}} \left(\frac{K}{K_{\text{bar}}} \right)^{1/2} e^{\beta U_0}, \quad (41)$$

where we used the definition of τ_{rel} in Eq. (36), the equipartition result for a harmonic potential $C_0 = k_B T / K$ and where K_{bar} is the absolute value of the potential curvature at the barrier top. For details of the saddle-point approximation see Appendix C. The energy relaxation time τ_{rel} can be determined for model systems or from experimental or simulation trajectories by the integral over the squared correlation function (determined in the free-energy well) according to Eq. (37). We see that the different potential shapes shown in Fig. 1 lead to distinct pre-exponential factors and a dependence on the barrier height U_0 for the case of a harmonic potential with an absorbing cusp in Fig. 1a. For potentials with rather similar curvatures K and K_{bar} in the well and at the barrier the factor $\sqrt{K/K_{\text{bar}}}$ is expected to be rather close to unity.

F. Explicit results for relaxation times

We consider the Mori GLE for the reaction coordinate (also called the position for simplicity) $x(t)$

$$m \ddot{x}(t) = -K x(t) - \int_{-\infty}^{\infty} ds \Gamma(s) \dot{x}(t-s) + F(t), \quad (42)$$

where m is the effective mass, defined as $m = k_B T / \langle \dot{x}^2 \rangle$, K is the stiffness of the harmonic potential, the memory kernel $\Gamma(t)$ is here (for simplifying the Fourier analysis) defined to be a single-sided function, i.e. $\Gamma(t) = 0$ for $t < 0$, and we have moved the projection time to minus infinity, such that the integration of the non-Markovian friction extends over the entire time domain (see Section II H for a discussion of how Eq. (42) follows from projection theory). The autocorrelation function of the orthogonal force is for a time-independent Hamiltonian given by

$$\langle F(t) F(t') \rangle = k_B T \Gamma(|t - t'|), \quad (43)$$

where averages in this Section are taken over the orthogonal-force distribution. Note that the Mori GLE

in Eq. (42) is an exact equation of motion for a general non-linear reaction coordinate, unless one approximates the orthogonal force $F(t)$ as Gaussian, as we do in this paper and as is appropriate for a Gaussian system. Fourier-transformation of Eq. (42) leads to

$$-m\omega^2\tilde{x}(\omega) = -K\tilde{x}(\omega) - \iota\omega\tilde{\Gamma}(\omega)\tilde{x}(\omega) + \tilde{F}(\omega), \quad (44)$$

from which the response of the position to the orthogonal force follows as

$$\tilde{x}(\omega) = \tilde{\chi}(\omega)\tilde{F}(\omega) \quad (45)$$

with the response function given by

$$\tilde{\chi}(\omega) = \left[K - m\omega^2 + \iota\omega\tilde{\Gamma}(\omega) \right]^{-1}. \quad (46)$$

From Eqs. (43) and (45) the Fourier transform of the correlation function $C(t) = \langle x(s)x(s+t) \rangle$ follows as

$$\begin{aligned} \frac{\tilde{C}(\omega)}{k_B T} &= \left[\tilde{\Gamma}(\omega) + \tilde{\Gamma}(-\omega) \right] \tilde{\chi}(\omega) \tilde{\chi}(-\omega) \\ &= \frac{\tilde{\Gamma}(\omega) + \tilde{\Gamma}(-\omega)}{\left| K - m\omega^2 + \iota\omega\tilde{\Gamma}(\omega) \right|^2} \\ &= \frac{\tilde{\chi}(-\omega)}{\iota\omega} - \frac{\tilde{\chi}(\omega)}{\iota\omega}, \end{aligned} \quad (47)$$

where the last equation follows directly from the definition of the response function in Eqs. (46) and where we used that $\chi(t)$ and $\Gamma(t)$ are real functions in the time domain. We define the derivative of the correlation function as

$$\begin{aligned} C_{xv}(t) &\equiv \frac{dC(t)}{dt} = \frac{d}{dt} \int \frac{d\omega}{2\pi} e^{\iota\omega t} \tilde{C}(\omega) \\ &= \int \frac{d\omega}{2\pi} e^{\iota\omega t} \iota\omega \tilde{C}(\omega), \end{aligned} \quad (48)$$

from which transpires that $\tilde{C}_{xv}(\omega) = \iota\omega\tilde{C}(\omega)$ and thus from Eqs. (47)

$$\frac{\tilde{C}_{xv}(\omega)}{k_B T} = \tilde{\chi}(-\omega) - \tilde{\chi}(\omega). \quad (49)$$

The time-domain response function $\chi(t)$ is a single-sided function, therefore the Fourier transform of the single-sided correlation function $C_{xv}^+(t) \equiv \theta(t)C_{xv}(t)$ is, if the response function $\chi(t)$ is regular in the limit $t \rightarrow 0$ (we will come back to this important condition when we discuss the massless non-Markovian scenario in Sec. II G) given by

$$\frac{\tilde{C}_{xv}^+(\omega)}{k_B T} = -\tilde{\chi}(\omega). \quad (50)$$

This is a useful result for analytical calculations, as the response function $\tilde{\chi}(\omega)$ has the minimal pole structure. From the time-domain function $C_{xv}^+(t)$ the single-sided

correlation function $C^+(t) \equiv \theta(t)C(t)$ is obtained by straightforward integration as

$$C^+(t) = -\theta(t) \int_t^\infty ds C_{xv}^+(s) = k_B T \theta(t) \int_t^\infty ds \chi(s), \quad (51)$$

which can then be used to calculate the relaxation time τ_{rel} according to Eq. (37). Note that the time-domain result in Eq. (51) is equivalent to the Fourier-domain result

$$\tilde{C}^+(\omega) = \frac{k_B T}{\iota\omega} (\tilde{\chi}(0) - \tilde{\chi}(\omega)). \quad (52)$$

In the following we will consider a single-exponential memory kernel

$$\Gamma(t) = \theta(t)\gamma e^{-t\tau}/\tau \quad (53)$$

with a memory time τ , whose Fourier transform is given by

$$\tilde{\Gamma}(\omega) = \frac{\gamma}{1 + \iota\tau\omega}. \quad (54)$$

1. Two-pole analysis for Markovian system: Kramers turnover

We first consider the Markov limit, obtained for vanishing memory time $\tau \rightarrow 0$, in which case the Fourier-transformed memory kernel in Eq. (54) reads $\tilde{\Gamma}(\omega) = \gamma$ and we are thus left with the damped harmonic oscillator model. The response function in Eq. (46) simplifies as

$$\tilde{\chi}(\omega) = \frac{1}{K - m\omega^2 + \iota\gamma\omega} = -\frac{1}{m(\omega - \omega_1)(\omega - \omega_2)} \quad (55)$$

with the two poles given by

$$\omega_{1,2} = \frac{\iota\gamma}{2m} \pm \left(\frac{K}{m} - \frac{\gamma^2}{4m^2} \right)^{1/2}. \quad (56)$$

We note that the two poles coincide if the argument of the square root vanishes, which happens at the crossover between the overdamped and underdamped regimes and in which case the correlation function decays single-exponentially, as announced earlier. The response function in the time domain follows from residual calculus as

$$\chi(t) = -\frac{\theta(t)}{m} \left(\frac{\iota e^{\iota\omega_1 t}}{\omega_1 - \omega_2} + \frac{\iota e^{\iota\omega_2 t}}{\omega_2 - \omega_1} \right) \quad (57)$$

with $\chi(t=0) = 0$, i.e., there is no instantaneous response for finite mass. The correlation function follows for positive times from Eq. (51) as

$$C^+(t) = \frac{\theta(t)k_B T}{m} \left(\frac{e^{\iota\omega_1 t}}{\omega_1(\omega_1 - \omega_2)} + \frac{e^{\iota\omega_2 t}}{\omega_2(\omega_2 - \omega_1)} \right), \quad (58)$$

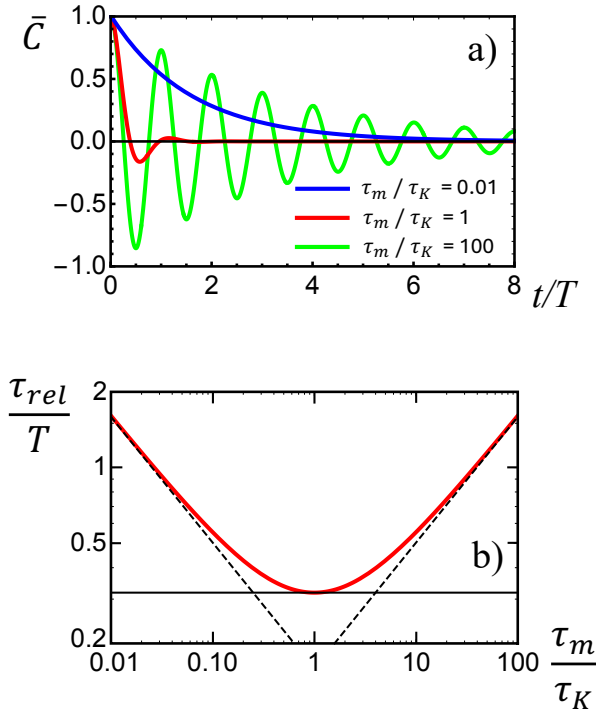


FIG. 2. Analytical results in the Markovian two-pole limit corresponding to vanishing memory time $\tau = 0$. a) Rescaled correlation function $\bar{C}(t) = C(t)/C_0$ according to Eqs. (58) and (59) and using the results for the poles in Eq. (56) for three different rescaled masses $\tau_m/\tau_K = mK/\gamma^2$, where $\tau_m = m/\gamma$ is the inertial relaxation time and $\tau_K = \gamma/K$ is the overdamped relaxation time. Time t is rescaled by the harmonic oscillation period in the frictionless limit $T = 2\pi\sqrt{m/K}$. b) Rescaled relaxation time τ_{rel}/T according to Eqs. (61) as function of the rescaled mass $\tau_m/\tau_K = mK/\gamma^2$. The asymptotic scalings in the high-mass limit (high τ_m/τ_K) $\tau_{\text{rel}} \sim m/\gamma$ and in the high-friction limit (small τ_m/τ_K) $\tau_{\text{rel}} \sim \gamma/K$ are indicated by straight broken lines. At the minimum at $\tau_m/\tau_K = mK/\gamma^2 = 1$ the relaxation time is given by $\tau_{\text{rel}} = T/\pi$, which corresponds to the transition-state-theory prediction.

from which the variance follows as

$$C_0 = 2C^+(0) = -\frac{k_B T}{m \omega_1 \omega_2} = \frac{k_B T}{K}, \quad (59)$$

in agreement with the equipartition theorem and where we used the convention for the Heaviside function that $\theta(0) = 1/2$. In Fig. 2a) we plot $\bar{C}(t) = C(t)/C_0$ for three different rescaled masses $\tau_m/\tau_K = mK/\gamma^2$ as a function of time t rescaled by the harmonic oscillation period $T = 2\pi\sqrt{m/K}$, where $\tau_m = m/\gamma$ is the inertial relaxation time and $\tau_K = \gamma/K$ is the overdamped relaxation time. We see that for small mass, $\tau_m/\tau_K = 0.01$ (blue line), the correlation function decays monotonically, for large mass, $\tau_m/\tau_K = 100$ (green line), long-range oscillations are visible, while for intermediate mass, $\tau_m/\tau_K = 1$ (red line), the decay is fastest and accompanied by only a few oscillations. It transpires that the relaxation time

Eq. (37) defined by the decay of the squared correlation function is minimal for intermediate mass (or intermediate friction).

From Eqs. (58) and (59) the energy relaxation time defined in Eq. (37) follows as

$$\tau_{\text{rel}} = -\frac{(\omega_1 + \omega_2)^2 + \omega_1 \omega_2}{i\omega_1 \omega_2 (\omega_1 + \omega_2)}. \quad (60)$$

By inserting Eq. (56) into Eq. (60) we obtain the relaxation time as

$$\tau_{\text{rel}} = \frac{\gamma}{K} + \frac{m}{\gamma}, \quad (61)$$

which is shown in Fig. 2b) and transparently displays the Kramers turnover: for large friction coefficient γ (small rescaled mass $\tau_m/\tau_K = mK/\gamma^2$) the relaxation time is linear in γ , and thus also the barrier-crossing time increases linear in γ , as follows from Eq. (27), while for small γ (large rescaled mass $\tau_m/\tau_K = mK/\gamma^2$) the relaxation time and thus the barrier-crossing time is proportional to $1/\gamma$. In between these two limits the relaxation time exhibits a minimum for a friction given by $\gamma^2 = mK$, at this minimum the relaxation time is given by $\tau_{\text{rel}} = 2\sqrt{m/K}$, which apart from a numerical factor is equivalent to the transition-state-theory prediction, as is explained in Appendix F.

The asymptotic behaviors captured by Eq. (61) follows from pole analysis: In the high-friction limit $\gamma^2 \gg mK$ we obtain from Eq. (56) $\omega_1 \simeq iK/\gamma$ and $\omega_2 \simeq i\gamma/m$. Since $\omega_1 \ll \omega_2$ we conclude that ω_1 describes the asymptotic long-time decay and thus is the dominant pole, we see from Eq. (61) that the relaxation time in the high-friction limit indeed is given by $\tau_{\text{rel}} \simeq i/\omega_1$. Since in the overdamped limit $m \rightarrow 0$ the only pole is ω_1 (as follows directly from Eq. (55)), it transpires that the correlation function $C(t)$ in this limit decays single-exponentially, thus the diffusivity in Eq. (28) is time-independent and our approach is exact since no cumulant expansion is needed; noteworthy, our approach is also exact at the crossover friction $\gamma^2 = 4mK$, since also here $C(t)$ decays single-exponentially.

In the low-friction limit $\gamma^2 \ll mK$ we obtain from Eq. (56) $\omega_{1,2} \simeq i\gamma/(2m) \pm \sqrt{K/m}$. The inverse imaginary part of $\omega_{1,2}$ sets the decay time, which diverges with increasing mass and dominates the relaxation time in Eq. (61), as visualized in Fig. 2. Note that in the underdamped limit $m \rightarrow \infty$ the decay of the correlation function does not become single-exponential and thus our cumulant-expansion approach is approximate.

2. Three-pole analysis for non-Markovian system: memory turnover

We now consider the response function in Eq. (46) with the single exponential memory kernel in Eq. (54) for finite memory time τ , which we rewrite in terms of

the three poles as

$$\begin{aligned}\tilde{\chi}(\omega) &= -\frac{1 + i\tau\omega}{im\tau(\omega^3 - i\omega^2/\tau - \omega(\gamma/\tau + K)/m + iK/(m\tau))} \\ &= -\frac{1 + i\tau\omega}{m\tau(\omega - \omega_1)(\omega - \omega_2)(\omega - \omega_3)}.\end{aligned}\quad (62)$$

Using the Cardano formula the poles are given as

$$\omega_i = \epsilon_i u_+ - \frac{p}{3\epsilon_i u_+} - \frac{b}{3}, \quad (63)$$

where $\epsilon_1 \equiv 1$, $\epsilon_{2,3} \equiv -1/2 \pm i\sqrt{3}/2$ are the complex three cubic roots of 1, $u_+ \equiv (-q/2 + (q^2/4 + p^3/27)^{1/2})^{1/3}$, $p \equiv c - b^2/3$, $q \equiv 2b^3/27 - cb/3 + d$, $b \equiv -i/\tau$, $c \equiv -\gamma/(\tau m) - K/m$, $d \equiv iK/(m\tau)$, for details see Appendix D. The response function in the time domain follows from residual calculus as

$$\chi(t) = -\frac{\theta(t)}{m\tau} \left(\frac{(1 + i\omega_1\tau)e^{i\omega_1 t}}{(\omega_1 - \omega_2)(\omega_1 - \omega_3)} + \frac{(1 + i\omega_2\tau)e^{i\omega_2 t}}{(\omega_2 - \omega_1)(\omega_2 - \omega_3)} + \frac{(1 + i\omega_3\tau)e^{i\omega_3 t}}{(\omega_3 - \omega_1)(\omega_3 - \omega_2)} \right), \quad (64)$$

from which the correlation function follows from Eq. (51) by integration as

$$C^+(t) = \frac{\theta(t)k_B T}{m\tau} \left(\frac{(\tau - i/\omega_1)e^{i\omega_1 t}}{(\omega_1 - \omega_2)(\omega_1 - \omega_3)} + \frac{(\tau - i/\omega_2)e^{i\omega_2 t}}{(\omega_2 - \omega_1)(\omega_2 - \omega_3)} + \frac{(\tau - i/\omega_3)e^{i\omega_3 t}}{(\omega_3 - \omega_1)(\omega_3 - \omega_2)} \right) \quad (65)$$

with the variance given as

$$C_0 = 2C^+(0) = -\frac{i k_B T}{m\tau \omega_1 \omega_2 \omega_3} = \frac{k_B T}{K}, \quad (66)$$

which again is the expected result from the equipartition theorem. In Fig. 3a) we plot $\bar{C}(t) = C(t)/C_0$ for three different rescaled memory times τ/τ_K as a function of time t rescaled by the oscillation period of the Markovian frictionless harmonic oscillator $T = 2\pi\sqrt{m/K}$ for fixed small rescaled mass $\tau_m/\tau_K = mK/\gamma^2 = 0.01$. We see that for small memory time, $\tau/\tau_K = 0.1$ (blue line), the correlation function decays almost purely exponentially, while for intermediate memory time, $\tau/\tau_K = 0.5$ (red line), pronounced oscillations are visible but the decay time of the envelope is not changed much. For long memory time, $\tau/\tau_K = 2$ (green line), we see that the

oscillation period has slightly changed and is now of the order of T , while the decay time of the envelope is increased considerably. In Appendix E we explain this behavior in terms of a pole analysis, where we show that the decay time of the exponential envelope in fact diverges as τ^2 for long memory times. These results show that for long memory time, the dynamics of the reaction coordinate becomes similar to a highly inertial system, as has been noted before based on simulation trajectories [63–66], meaning that the effect of friction is effectively reduced. The presence of oscillations with a period of T suggests that a finite system mass m is crucial in order to correctly account for the effects of long memory times, as will be discussed in more detail in Sec. II G.

From Eqs. (65) and (66) the relaxation time defined in Eq. (37) follows as

$$\tau_{\text{rel}} = \frac{2K^2}{m^2\tau^2} [I_1(\omega_1, \omega_2, \omega_3) + I_2(\omega_1, \omega_2, \omega_3) + I_1(\omega_2, \omega_3, \omega_1) + I_2(\omega_2, \omega_3, \omega_1) + I_1(\omega_3, \omega_1, \omega_2) + I_2(\omega_3, \omega_1, \omega_2)], \quad (67)$$

where we defined the functions

$$I_1(\omega_1, \omega_2, \omega_3) \equiv \frac{i(\tau - i/\omega_1)^2}{2\omega_1(\omega_1 - \omega_2)^2(\omega_1 - \omega_3)^2}, \quad (68)$$

$$I_2(\omega_1, \omega_2, \omega_3) \equiv -\frac{2i(\tau - i/\omega_2)(\tau - i/\omega_3)}{(\omega_2 + \omega_3)(\omega_2 - \omega_1)(\omega_3 - \omega_1)(\omega_2 - \omega_3)^2}. \quad (69)$$

In the zero-mass limit $m \rightarrow 0$, Eq. (67) yields

$$\tau_{\text{rel}} = \frac{\gamma}{K} \left(\frac{1 + (\tau K/\gamma)^3}{1 + \tau K/\gamma} \right). \quad (70)$$

with the limits given by

$$\tau_{\text{rel}} \simeq \begin{cases} \gamma/K - \tau & , \tau \ll \gamma/K \\ \tau^2 K/\gamma & , \tau \gg \gamma/K, \end{cases} \quad (71)$$

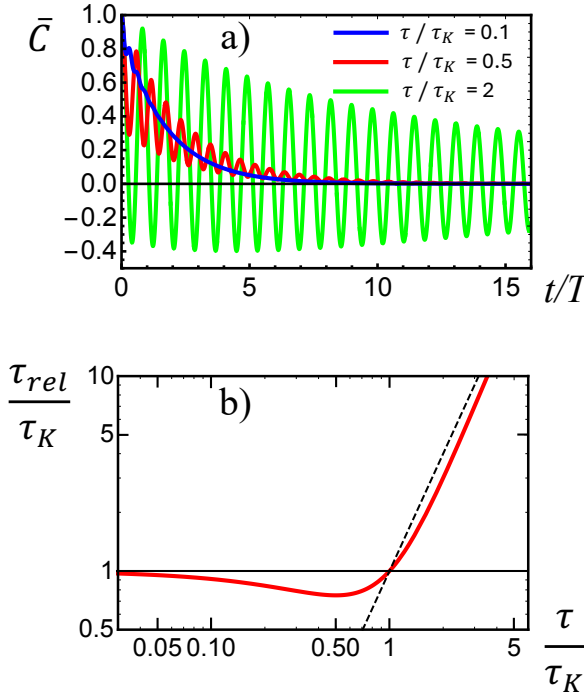


FIG. 3. Analytical results for the non-Markovian three-pole scenario for finite memory time τ . a) Rescaled correlation function $\bar{C}(t) = C(t)/C_0$ according to Eqs. (65) and (66) using the results for the poles in Eq. (63) for three different rescaled memory times τ/τ_K , where $\tau_K = \gamma/K$ is the over-damped Markovian relaxation time. Time t is rescaled by the Markovian harmonic oscillation period in the frictionless limit $T = 2\pi\sqrt{m/K}$ and the rescaled mass is set to a small value of $\tau_m/\tau_K = mK/\gamma^2 = 0.01$. b) Rescaled relaxation time τ_{rel}/τ_K in the zero-mass limit according to Eqs. (70) as function of the rescaled memory time τ/τ_K . The asymptotic scaling in the long-memory-time limit $\tau_{\text{rel}} \sim \tau^2$ is indicated by a straight broken line.

see Appendix E for details. So we obtain for small memory times τ a reduction of τ_{rel} that is linear in τ , which leads to the memory-induced speed-up of barrier-crossing times, while for large memory times τ_{rel} increases quadratically with τ , which leads to memory-induced barrier-crossing slow-down. The memory-induced speed-up term we obtain in Eq. (67) for small τ is in exact agreement with the zero-mass prediction of GH theory, as demonstrated in Appendix F, however, the turnover to the memory-induced barrier-crossing slow-down is missed by GH theory. This salient memory-turnover behavior is illustrated in Fig. 3b, where we plot Eq. (70) as a function of the rescaled memory time τ/τ_K . The minimum of τ_{rel} appears for memory time $\tau^* = \gamma/(2K)$, so we see that in the limit of a vanishing confining harmonic potential, i.e. for $K \rightarrow 0$, our Gaussian analysis predicts the minimum of the relaxation time to move to infinite memory time. This might explain why GH theory, which treats the escape over a barrier without relaxation in a well, does not yield a minimum of the relaxation

time and also not the long-memory-time slow-down of the barrier-crossing rate. For memory times $\tau \gg \tau^*$ the relaxation time exhibits a quadratic increase. This increase of the relaxation time is reflected by the slow decay of the correlation function envelope visible in Fig. 3a for long memory times. When taking the $m \rightarrow 0$ limit of the correlation function Eq. (65) before calculating the relaxation time according to Eq. (37) one misses the long-time barrier-crossing slow-down, as shown in Sec. II G, which demonstrates that the barrier-crossing slow down for long memory time originates from the interplay between the three poles and involves a finite mass.

If instead of using $p = 2$ for calculating the moments according to Eq. (31) one takes $p = 1$, the relaxation time is instead of Eq. (67) given by an integral over the correlation function $\tau_{\text{rel}}^{p=1} = \int_0^\infty dt \bar{C}(t) = \int_0^\infty dt C(t)/C_0$. From Eqs. (47) we obtain $\int_0^\infty dt C(t) = \bar{C}(\omega = 0)/2 = k_B T \gamma / K^2$, together with $C_0 = k_B T / K$ we thus obtain $\tau_{\text{rel}}^{p=1} = \gamma / K$ independent of mass and of memory time. So we see that when defining the relaxation time as the integral over the correlation function, inertial and non-Markovian effects are completely missed, while using $p = 2$ and thus defining the relaxation as the integral over the correlation function squared, which corresponds to the energy-energy correlation function, non-Markovian effects are accounted for. This is easy to understand, since, as shown in Figs. 2(a) and 3(a), for large mass and large memory time oscillations appear in the correlation function and the integral over the correlation does not reflect the decay time of the exponential envelope.

G. The mass-less non-Markovian system with single-exponential memory is singular

We reconsider the response function in Eq. (46) with the single exponential memory kernel in Eq. (54) but already now take the mass-less limit $m \rightarrow 0$, in which case we obtain

$$\begin{aligned} \tilde{\chi}_{m=0}(\omega) &= \frac{1}{K + i\gamma\omega / (1 + i\tau\omega)} = \frac{1 + i\tau\omega}{K + i\omega(\gamma + \tau K)} \\ &= \frac{-i\gamma}{(\gamma + \tau K)^2(\omega - iK/(\gamma + \tau K))} + \frac{\tau}{\gamma + K\tau}, \end{aligned} \quad (72)$$

where in the last line we separated off a constant so that the remainder of the response function decays to zero for $\omega \rightarrow \infty$. Using this separation, the response function in the time domain is straightforwardly obtained as

$$\chi_{m=0}(t) = \theta(t) \frac{\gamma}{(\gamma + \tau K)^2} e^{-tK/((\gamma + \tau K))} + \frac{\tau}{\gamma + K\tau} \delta(t). \quad (73)$$

We see that the response function exhibits a very unusual delta-peak response at zero time. This singularity is a result of neglecting the mass in the presence of a finite memory time, which transpires from the fact that the

delta peak vanishes for $\tau \rightarrow 0$. As a consequence of the presence of this singularity, the separation of the Fourier transform of the antisymmetric position-velocity correlation function $\tilde{C}_{xv}(\omega)$ in Eq. (49) into the single-sided function $\tilde{C}_{xv}^+(\omega)$ in Eq. (50) is not possible. Instead, we use Eq. (47) to calculate $\tilde{C}(\omega)$ from Eq. (73) and obtain after back Fourier transformation

$$C_{m=0}(t) = \frac{k_B T}{K(1 + \tau K/\gamma)} e^{-|t|K/((\gamma + \tau K)} \quad (74)$$

The variance follows from this expression as $C_{m=0}(0) = k_B T / (K(1 + \tau K/\gamma))$, in stark contrast to the equipartition-theorem prediction $C(0) = k_B T / K$ obtained from the three-pole analysis in Eq. (66), which is a consequence of neglecting the regularizing mass in the starting equation, as has been pointed out before [69]. From Eq. (74) the relaxation time defined in Eq. (37) follows as $\tau_{\text{rel}}^{m=0} = (\gamma/K)(1 + \tau K/\gamma)$, which predicts a linear increase of the relaxation with memory time τ , very different from the result from the full three-pole analysis in Eq. (70). A heuristic fix is possible by rescaling the result for the relaxation time by the ratio of the mass-less and the actual variances according

to $(C_{m=0}(0)/C(0))^2 \tau_{\text{rel}}^{m=0} = (\gamma/K)/(1 + \tau K/\gamma)$, which correctly recovers the intermediate memory acceleration regime but misses the long-memory slow-down regime in Eq. (70). We conclude that in order to correctly predict barrier-crossing dynamics one needs to keep a finite mass in the equation of motion describing the reaction-coordinate dynamics.

H. The zero-memory-time limit of the GLE is time-reversible

After having shown that the zero-mass limit of the GLE is singular, we now discuss the zero-memory-time limit $\tau \rightarrow 0$ of the GLE and show that in this limit also a singularity arises, which in fact is crucial in order to preserve time reversibility of the resulting Langevin equation. This resolves the puzzling finding that in its usual formulation, the Langevin equation breaks time-reversal symmetry, while the GLE, which is derived by exact projection from Hamilton's equation of motion, obeys time-reversal symmetry (as Hamilton dynamics does).

To clarify this issue, we consider the Mori GLE in the form obtained by projection formalism [18, 68], which reads [70]

$$\ddot{B}(w, t) = -K_M(B(w, t) - \langle B \rangle) - \int_0^{t-t_P} ds \Gamma_M(s) \dot{B}(w, t-s) + F_M(w, t). \quad (75)$$

Note that in contrast to the GLE Eq. (42) we have been using to derive all explicit results so far, the Heisenberg observable $B(w, t)$ and the orthogonal force $F_M(w, t)$ in Eq. (75) have an explicit dependence on the $6N$ -dimensional phase-space variable $w = (\{\mathbf{r}_N\}, \{\mathbf{p}_N\})$, where N denotes the number of particles and $\{\mathbf{r}_N\}$ are the particle positions and $\{\mathbf{p}_N\}$ the particle momenta in three-dimensional space. Time reversibility means that the trajectory of a many-body system is invariant when time and momenta are inverted. The Hamilton equations of motion are time-reversible for a Hamiltonian that is even in the momenta $\{\mathbf{p}_N\}$. Note that eq. (75) results from an exact derivation and therefore must also be time-reversible. The time at which the projection is taking place, t_P , appears explicitly in Eq. (75) [70]. Eq. (42) is obtained from Eq. (75) by i) pushing the propagation time in Eq. (75) infinitely far into the past, $t_P \rightarrow -\infty$, which produces the time ordering $t > t_P$ and makes the upper integral boundary in Eq. (75) equal to $+\infty$, ii) defining mass-rescaled parameters $\Gamma(t) = m\theta(t)\Gamma_M(t)$, $K = mK_m$ and $F(t) = mF_M(w, t)$, where we defined the memory kernel $\Gamma(t)$ to be single-sided so that the integration range of the friction term can be extended to the negative time domain, iii) introducing a shifted observable $x(t) = B(w, t) - \langle B \rangle$ and skipping the phase-space

dependence of $x(t)$ and $F(t)$.

Setting $t_P = 0$ in the remainder, time reversibility around $t = 0$ manifests for the Heisenberg observable as

$$\begin{aligned} \ddot{B}(\{\mathbf{r}_N\}, \{\mathbf{p}_N\}, t) &= \ddot{B}(\{\mathbf{r}_N\}, -\{\mathbf{p}_N\}, -t) \\ \dot{B}(\{\mathbf{r}_N\}, \{\mathbf{p}_N\}, t) &= -\dot{B}(\{\mathbf{r}_N\}, -\{\mathbf{p}_N\}, -t) \\ B(\{\mathbf{r}_N\}, \{\mathbf{p}_N\}, t) &= B(\{\mathbf{r}_N\}, -\{\mathbf{p}_N\}, -t). \end{aligned} \quad (76)$$

Using the time-reversal symmetry of $\Gamma_M(t)$, i.e. $\Gamma_M(t) = \Gamma_M(-t)$, we obtain

$$\begin{aligned} &\int_0^t ds \Gamma_M(s) \dot{B}(\{\mathbf{r}_N\}, \{\mathbf{p}_N\}, t-s) \\ &= \int_0^{-t} ds \Gamma_M(s) \dot{B}(\{\mathbf{r}_N\}, -\{\mathbf{p}_N\}, -t-s), \end{aligned} \quad (77)$$

thus the memory-friction term satisfies time-reversal symmetry as well. Since the left side and the first two terms of the right side of Eq. (75) are time-reversible, realizing that K_M is independent of time and momenta, the orthogonal force must also be time-reversible since the entire equation is, we therefore conclude

$$F(\{\mathbf{r}_N\}, \{\mathbf{p}_N\}, t) = F(\{\mathbf{r}_N\}, -\{\mathbf{p}_N\}, -t). \quad (78)$$

Thus not only the GLE as an equation is time-reversible, in fact each individual term of the GLE is time-reversible as well, which is a much stronger statement. For details and derivations see Appendix G,

In the Markovian limit the memory kernel becomes infinitely short-ranged and can be written as

$$\Gamma_M(t) = 2\gamma_M\delta(t). \quad (79)$$

Using that

$$\begin{aligned} & \int_0^t ds \Gamma_M(s) \dot{B}(w, t-s) \\ &= 2\gamma_M \int_0^t ds \delta(s) \dot{B}(w, t-s) \\ &= 2\gamma_M \dot{B}(w, t) \int_0^t ds \delta(s) = \gamma_M \dot{B}(w, t) \text{sig}(t), \end{aligned} \quad (80)$$

we obtain in the Markovian limit the Langevin equation as

$$\ddot{B}(w, t) = -K_M(B(w, t) - \langle B \rangle) - \gamma_M \text{sig}(t) \dot{B}(w, t) + F_M(w, t), \quad (81)$$

where $\text{sig}(t)$ is the signum function with $\text{sig}(t) = 1$ for $t > 0$ and $\text{sig}(t) = -1$ for $t < 0$. Obviously, the Langevin equation in Eq. (81), obeys time-reversal symmetry around $t = 0$ but exhibits a discontinuity of the friction term at the time origin, $t = 0$, which reflects the fact that the friction term in the underlying GLE in Eq. (75) vanishes for $t - t_P = 0$. We note that this discontinuity of the friction term in the Langevin Eq. (81) is unproblematic when considering time-averaged quantities. We therefore not only show in Sec. II G that the zero-mass limit is ill-defined for non-Markovian friction kernels (at least for the single-exponential kernel we consider in this paper), we also show here that in the zero-memory-time limit the resulting Langevin equation is time-reversible and contains a discontinuity which, when neglected, breaks time-reversal symmetry.

III. CONCLUSIONS AND DISCUSSION

Using an exact mapping of the Green function of a Gaussian general non-Markovian reaction coordinate x onto a generalized Fokker Planck equation with a time-dependent diffusivity, we derive an expression of the mean-first passage to reach x_f starting from $x_0 < x_f$ which, combining Eqs. (27), (36), (37), reads

$$\tau_{\text{mfp}} = \frac{\tau_{\text{rel}}}{C_0} \int_{x_0}^{x_f} dx e^{\beta U(x)} \int_{x_{\text{ref}}}^x dx' e^{-\beta U(x')}. \quad (82)$$

In this expression $x_{\text{ref}} < x_0$ is the position of a reflecting boundary, $C_0 = C(t=0) = \langle x^2 \rangle$ is the mean-square position of the reaction coordinate and τ_{rel} denotes the

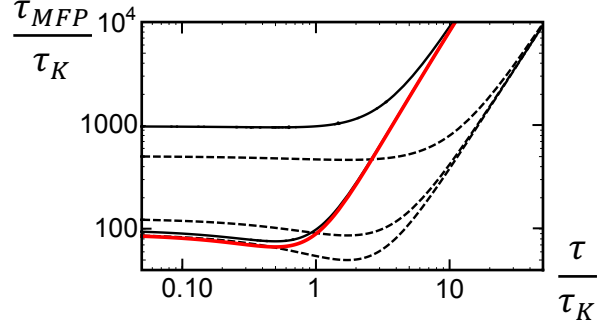


FIG. 4. Comparison of our analytical results (Eqs. (84), (85) and (67), black solid lines, Eqs. (84), (85) and (70), red solid line) and a previous fit of a scaling function to simulation results (Eq. 8 in [71], broken lines) for the well-to-barrier-top mean-first passage time (rescaled by $\tau_K = \gamma/K$) of the non-Markovian model with single-exponential memory, all for a barrier height of $U_0 = 3k_B T$. Results are shown for three different values of the rescaled mass $\tau_m/\tau_K = mK/\gamma^2 = 10, 0.1, 0$ (from top to bottom) as a function of the memory time rescaled by $\tau_K = \gamma/K$.

relaxation time given by an integral over the squared positional correlation function $C(t) = \langle x(0)x(t) \rangle$ according to

$$\tau_{\text{rel}} = \frac{2}{C_0^2} \int_0^\infty dt C^2(t). \quad (83)$$

The derivation is exact for a harmonic potential $U(x) = Kx^2/2$ and for a correlation function $C(t)$ that decays single-exponentially, for general $C(t)$ Eq. (83) correspond to the first term of a systematic cumulant expansion. Employing a saddle point approximation on the double-integral in Eq. (82) we obtain the Arrhenius-type expression in terms of the exponential of the barrier height U_0

$$\tau_{\text{mfp}} = \tau_{\text{rel}} \Theta e^{\beta U_0}, \quad (84)$$

where Θ is a unitless factor that depends on the potential shape. For the three scenarios shown in Fig. 1 it is given by (Eqs. (39), (40), (41))

$$\Theta = \begin{cases} \sqrt{\frac{\pi}{\beta U_0}} & \text{scenario Fig.1a} \\ \pi \left(\frac{K}{K_{\text{bar}}} \right)^{1/2} & \text{scenario Fig.1b} \\ 2\pi \left(\frac{K}{K_{\text{bar}}} \right)^{1/2} & \text{scenario Fig.1c.} \end{cases} \quad (85)$$

One key feature of our theory, which distinguishes it from other theories, is that memory and inertial effects are fully included and enter via the two-point autocorrelation function $C(t)$, which from simulations and experiments can be much more easily determined than the memory function. In Fig. 2b we demonstrate that the so-called Kramers turnover, i.e. the minimum of the barrier-crossing time of a Markovian system for intermediate friction and the asymptotic scaling in the

high and low friction limits, $\tau_{\text{mfp}} \sim (\gamma/K)e^{\beta U_0}$ and $\tau_{\text{mfp}} \sim (m/\gamma)e^{\beta U_0}$ are correctly reproduced. In Fig. 3b we demonstrate that also the more complex memory turnover, i.e. the minimum of the barrier-crossing time for intermediate memory time τ and the asymptotic scaling $\tau_{\text{mfp}} \sim \tau^2 e^{\beta U_0}$, are correctly reproduced. It is noteworthy that our theory reproduces exactly the GH theory in the zero-mass small-memory-time limit but, in contrast to GH theory, also correctly reproduces the large-memory-time limit.

In Fig. 4 we perform a quantitative comparison for the mean-first passage time to reach from the well minimum to the barrier top (scenario Fig. 1b) predicted by our theory with extensive simulation data for a double-well potential and a single-exponential kernel [71]. The mean-first passage times in the simulations are obtained from long trajectories by calculating the mean all-to-first passage times, i.e. counting all recrossings of the starting position, which has been shown to correspond to the escape time from a well, which is the quantity predicted by reaction rate theories [72]. We compare our theory (Eqs. (84), second line of (85) and (67), black solid lines, Eqs. (84), second line of (85) and (70), red solid line) for three different values of the rescaled mass $\tau_m/\tau_K = mK/\gamma^2 = 10, 0.1, 0$ (from top to bottom) with a scaling function calibrated to simulation results (Eq. 8 in [71], broken lines). The simulations were done for a double well potential of the form $U(x) = U_0(x^2/L^2 - 1)^2$, for which $K/K_{\text{bar}} = 2$, we use $U_0 = 3k_B T$ in Fig. 4 since the simulations were mostly done around that barrier energy. We see that our theory and the simulation data agree well for low memory time and low mass, which reflects that in this limit our theory becomes exact. For large mass and long memory times there are deviations, yet, our theory reproduces the memory turnover, that means the minimum in τ_{mfp} as a function of τ , rather well.

The deviations between our theoretical predictions (solid lines) and the previously published simulation results (broken lines) in Fig. 4 stem from two approximations we employed. First, our derivation is exact for a harmonic potential and treats the barrier as an absorbing cusp, as illustrated in Fig. 1a. We obtain on the harmonic level a separation between potential and memory/inertial effects, as seen in Eqs. (82), for non-harmonic potentials we expect a coupling between non-harmonicities and memory effects, which could be studied in simulations. Secondly, our derivation is exact for single-exponential correlation functions $C(t)$ and treats

more complex correlation functions by a systematic cumulant expansion to first order (see Sec. IID). As Fig. 3b demonstrates, for long memory time τ the correlation function even for single-exponential memory kernels does not decay single-exponentially but exhibits an oscillating-exponential decay. In future extensions of our theory, it would be interesting to go beyond the first-order cumulant expansion.

ACKNOWLEDGMENTS

We acknowledge support by Deutsche Forschungsgemeinschaft Grant CRC 1449 "Dynamic Hydrogels at Biointerfaces", Project ID 431232613, Projects A02 and A03.

Appendix A: Derivation of the Green function

The condition in Eq. (2) that the joint distribution is symmetric leads to $c(t) = a(t)$. The normalization in Eq. (3) leads to

$$\mathcal{N} = \frac{2\pi}{\sqrt{a^2(t) - b^2(t)}}. \quad (\text{A1})$$

The definition of the two-point autocorrelation function $C(t)$ in Eq. (4) leads to

$$C(t) = -\frac{b(t)}{a^2(t) - b^2(t)}. \quad (\text{A2})$$

The definition of the variance C_0 in Eq. (5) leads to

$$C_0 = \frac{a(t)}{a^2(t) - b^2(t)}. \quad (\text{A3})$$

Inversion of these equations leads to

$$a(t) = \frac{1}{C_0(1 - \bar{C}^2(t))} \quad (\text{A4})$$

and

$$b(t) = -\frac{\bar{C}(t)}{C_0(1 - \bar{C}^2(t))}, \quad (\text{A5})$$

where we used the rescaled correlation function $\bar{C}(t)$ defined in Eq. (7) and from which Eq. (6) follows.

Appendix B: Derivation of the generalized Fokker-Planck equation

By taking a time derivative of Eq. (9) we obtain

$$\frac{\partial \mathcal{P}(x, t|x_0)}{\partial t} = \frac{\bar{C}'(t) \left((x - \bar{C}(t)x_0) x_0 \bar{C}(t) (1 - \bar{C}^2(t)) - (x - \bar{C}(t)x_0)^2 \bar{C}^2(t) + (1 - \bar{C}^2(t)) C_0 \bar{C}^2(t) \right)}{C_0 \bar{C}(t) (1 - \bar{C}^2(t))^2} \mathcal{P}(x, t|x_0), \quad (\text{B1})$$

where $\bar{C}'(t)$ denotes the derivate of $\bar{C}(t)$. With the first and second spatial derivatives of Eq. (9),

$$\frac{\partial \mathcal{P}(x, t|x_0)}{\partial x} = -\frac{(x - \bar{C}(t)x_0)}{C_0 (1 - \bar{C}^2(t))} \mathcal{P}(x, t|x_0), \quad (\text{B2})$$

$$\frac{\partial^2 \mathcal{P}(x, t|x_0)}{\partial x^2} = \left(-\frac{1}{C_0 (1 - \bar{C}^2(t))} + \frac{(x - \bar{C}(t)x_0)^2}{C_0^2 (1 - \bar{C}^2(t))^2} \right) \mathcal{P}(x, t|x_0), \quad (\text{B3})$$

we obtain by comparison with Eq. (B1)

$$\frac{\partial \mathcal{P}(x, t|x_0)}{\partial t} = -\frac{\bar{C}'(t)}{\bar{C}(t)} \mathcal{P}(x, t|x_0) - x \frac{\bar{C}'(t)}{\bar{C}(t)} \frac{\partial \mathcal{P}(x, t|x_0)}{\partial x} - \frac{C_0 \bar{C}'(t)}{\bar{C}(t)} \frac{\partial^2 \mathcal{P}(x, t|x_0)}{\partial x^2} \quad (\text{B4})$$

which is equivalent to Eq. (10).

Appendix C: Saddle-point approximation of the mean-first passage time for different potential shapes

To first order in the cumulant expansion introduced in Section II D, the mean-first passage time to reach the final position x_f for the first time when starting from x_0 follows from Eq. (27) as

$$\tau_{\text{mfp}} = D_0^{-1} \int_{x_0}^{x_f} dx e^{\beta U(x)} \int_{x_{\text{ref}}}^x dx' e^{-\beta U(x')}. \quad (\text{C1})$$

For high barriers, this double integral can be estimated using the saddle-point approximation. Let us first consider the scenario depicted in Fig. 1c, where the initial position x_0 is located to the left of the barrier and the final position x_f is located to the right of the barrier. We write

$$\tau_{\text{mfp}} = D_0^{-1} \int_{x_0}^{x_f} dx e^{\beta U(x)} I(x). \quad (\text{C2})$$

Since the integral over x includes the barrier, the exponential function in the integrand is maximal at the barrier position $x = x_{\text{max}}$, we therefore expand the function $I(x)$ around $x = x_{\text{max}}$ and obtain to first order

$$\begin{aligned} I(x) &\equiv \int_{x_{\text{ref}}}^x dx' e^{-\beta U(x')} \\ &= I(x_{\text{max}}) + (x - x_{\text{max}}) I'(x_{\text{max}}) + \dots \\ &= \int_{x_{\text{ref}}}^{x_{\text{max}}} dx' e^{-\beta U(x')} + (x - x_{\text{max}}) e^{-\beta U(x_{\text{max}})} + \dots \end{aligned} \quad (\text{C3})$$

The integrand is maximal at the minimum in the left well x_{min} , which is included in the integral for $x_{\text{ref}} < x_{\text{min}} <$

x_{max} . Assuming a high barrier and correspondingly a deep minimum in the well, the integral boundaries can be pushed to infinity and the potential can be expanded to second order around the minimum, so that we obtain

$$\begin{aligned} I(x) &\simeq \int_{-\infty}^{\infty} dx' e^{-\beta U(x')} + (x - x_{\text{max}}) e^{-\beta U(x_{\text{max}})} + \dots \\ &\simeq \int_{-\infty}^{\infty} dx' e^{-\beta U(x_{\text{min}}) - \beta K(x' - x_{\text{min}})^2/2} \\ &\quad + (x - x_{\text{max}}) e^{-\beta U(x_{\text{max}})} + \dots \\ &\simeq e^{-\beta U(x_{\text{min}})} \sqrt{\frac{2\pi}{\beta K}}, \end{aligned} \quad (\text{C4})$$

where we neglected the term proportional to $e^{-\beta U(x_{\text{max}})}$ since for large barriers it is negligible compared to the term proportional to $e^{-\beta U(x_{\text{min}})}$. To leading order $I(x)$ thus is a constant and we obtain for Eq. (C2)

$$\tau_{\text{mfp}} \simeq D_0^{-1} e^{-\beta U(x_{\text{min}})} \sqrt{\frac{2\pi}{\beta K}} \int_{x_0}^{x_f} dx e^{\beta U(x)}. \quad (\text{C6})$$

We now expand the argument of the exponential in the integrand around its maximum at x_{max} and extend the integration boundaries to plus and minus infinity, after which we obtain

$$\begin{aligned} \tau_{\text{mfp}} &\simeq D_0^{-1} e^{-\beta U(x_{\text{min}})} \sqrt{\frac{2\pi}{\beta K}} \\ &\quad \times \int_{-\infty}^{\infty} dx e^{\beta U(x_{\text{max}}) - \beta K_{\text{bar}}(x - x_{\text{max}})^2/2} \\ &\simeq \frac{2\pi}{\beta D_0 \sqrt{KK_{\text{bar}}}} e^{\beta U_0}, \end{aligned} \quad (\text{C7})$$

where K_{bar} denotes the absolute value of the curvature at the barrier and $U_0 \equiv U(x_{\max}) - U(x_{\min})$ is the barrier height. Using $D_0 = C_0/\tau_{\text{rel}}$ and $C_0 = k_B T/K$ this is equivalent to Eq. (41).

We now consider the scenario in Fig. 1b, where the initial position x_0 is located to the left of the barrier and the final position $x_f = x_{\max}$ is located right at the barrier. We rewrite Eq. (C1) as

$$\tau_{\text{mfp}} = D_0^{-1} \int_{x_0}^{x_{\max}} dx e^{\beta U(x)} I(x). \quad (\text{C8})$$

To leading order $I(x)$ is again given by Eq. (C4) so we obtain for Eq. (C2)

$$\tau_{\text{mfp}} \simeq D_0^{-1} e^{-\beta U(x_{\min})} \sqrt{\frac{2\pi}{\beta K}} \int_{x_0}^{x_{\max}} dx e^{\beta U(x)}. \quad (\text{C9})$$

We again expand the argument of the exponential in the integrand around its maximum at x_{\max} and extend the lower integration boundary to minus infinity, after which we obtain

$$\begin{aligned} \tau_{\text{mfp}} &\simeq D_0^{-1} e^{-\beta U(x_{\min})} \sqrt{\frac{2\pi}{\beta K}} \\ &\quad \times \int_{-\infty}^{x_{\max}} dx e^{\beta U(x_{\max}) - \beta K_{\text{bar}}(x - x_{\max})^2/2} \\ &\simeq \frac{\pi}{\beta D_0 \sqrt{K K_{\text{bar}}}} e^{\beta U_0}, \end{aligned} \quad (\text{C10})$$

which using $D_0 = C_0/\tau_{\text{rel}}$ and $C_0 = k_B T/K$ is equivalent to Eq. (40).

We now consider the harmonic scenario in Fig. 1a, where both initial position x_0 and final position $x_f > x_0$ are located in a harmonic potential well $U(x) = Kx^2/2$. We rewrite Eq. (C1) as

$$\tau_{\text{mfp}} = D_0^{-1} \int_{x_0}^{x_f} dx e^{\beta U(x)} I(x). \quad (\text{C11})$$

To leading order $I(x)$ is again given by Eq. (C4) so we obtain for Eq. (C2)

$$\tau_{\text{mfp}} \simeq D_0^{-1} \sqrt{\frac{2\pi}{\beta K}} \int_{x_0}^{x_f} dx e^{\beta U(x)}, \quad (\text{C12})$$

where we used that $U(x_{\min}) = 0$. We expand the argument of the exponential in the integrand to first order around x_f and extend the lower integration boundary to minus infinity, after which we obtain

$$\begin{aligned} \tau_{\text{mfp}} &\simeq D_0^{-1} \sqrt{\frac{2\pi}{\beta K}} \int_{-\infty}^{x_f} dx e^{\beta U(x_f) + \beta(x - x_f)U'(x_f)} \\ &\simeq \frac{1}{D_0 \beta U'(x_f)} \sqrt{\frac{2\pi}{\beta K}} e^{\beta U_0} \simeq \frac{1}{D_0 \beta K} \sqrt{\frac{\pi}{\beta U_0}} e^{\beta U_0} \end{aligned} \quad (\text{C13})$$

where we used $U(x_f) = U_0$, $U'(x_f) = Kx_f = \sqrt{2U_0 K}$ and which is, using $D_0 = C_0/\tau_{\text{rel}}$ and $C_0 = k_B T/K$, equivalent to Eq. (39).

Appendix D: Three-pole analysis using Cardano equation

The three poles are determined from Eq. (62) by the equation

$$\omega^3 + b\omega^2 + c\omega + d = 0 \quad (\text{D1})$$

with $b \equiv -i/\tau$, $c \equiv -\gamma/(\tau m) - K/m$, $d \equiv iK/(m\tau)$. Inserting the definition $\omega = t - b/3$ into Eq. (D1) leads to

$$t^3 + pt + q = 0 \quad (\text{D2})$$

with $p \equiv c - b^2/3$, $q \equiv 2b^3/27 - cb/3 + d$. Inserting now the definition $t = u - p/(3u)$, Eq. (D2) reduces to

$$u^6 + qu^3 - p^3/27 = 0, \quad (\text{D3})$$

which is a quadratic equation for u^3 with the two solutions

$$u_{\pm}^3 = -\frac{q}{2} \pm \sqrt{\frac{q^2}{4} + \frac{p^3}{27}}. \quad (\text{D4})$$

Taking the cubic root we obtain a total of six possible solutions

$$u_{i\pm} = \epsilon_i u_{\pm} = \epsilon_i \left[-\frac{q}{2} \pm \sqrt{\frac{q^2}{4} + \frac{p^3}{27}} \right]^{1/3}, \quad (\text{D5})$$

where $\epsilon_1 \equiv 1$, $\epsilon_{2,3} \equiv -1/2 \pm i\sqrt{3}/2$ are the complex three cubic roots of 1. To show that there are actually only three distinct solutions of Eq. (D3), we first realize that

$$u_+^3 = -\frac{p^3}{27u_-^3}, \quad (\text{D6})$$

from which follows that

$$u_+ = -\epsilon_j \frac{p}{3u_-}. \quad (\text{D7})$$

From the definition $t = u - p/(3u)$ we obtain from the positive-root solutions $\epsilon_i u_+$ of Eq. (D3) three solutions of Eq. (D2) as

$$t_i = \epsilon_i u_+ - \frac{p}{3\epsilon_i u_+}. \quad (\text{D8})$$

Inserting Eq. (D7) into Eq. (D8) we obtain

$$t_i = -\epsilon_i \epsilon_j \frac{p}{3u_-} + \frac{u_-}{\epsilon_i \epsilon_j} \quad (\text{D9})$$

where $j = 1, 2, 3$ is arbitrary. Using the relations

$$\begin{aligned} \epsilon_1 \epsilon_1 &= \epsilon_1 = 1/\epsilon_1 \\ \epsilon_2 \epsilon_2 &= \epsilon_3 = 1/\epsilon_2 \\ \epsilon_3 \epsilon_3 &= \epsilon_2 = 1/\epsilon_3 \\ \epsilon_1 \epsilon_2 &= \epsilon_2 = 1/\epsilon_3 \\ \epsilon_1 \epsilon_3 &= \epsilon_3 = 1/\epsilon_2 \\ \epsilon_2 \epsilon_3 &= \epsilon_1 = 1/\epsilon_1, \end{aligned} \quad (\text{D10})$$

it immediately follows from comparing Eq. (D8) and Eq. (D9) that

$$t_i = \epsilon_i u_+ - \frac{p}{3\epsilon_i u_+} = \epsilon_k u_- - \frac{p}{3\epsilon_k u_-} \quad (\text{D11})$$

where $k = 1, 2, 3$ is determined from the values of i and j according to the relations in Eq. (D10). We conclude from Eq. (D11) that there are only three distinct solutions of Eq. (D2) which can, without loss of generality, be expressed using the positive root u_+ given in Eq. (D8). From the definition $\omega = t - b/3$ we finally obtain for the poles

$$\omega_i = \epsilon_i u_+ - \frac{p}{3\epsilon_i u_+} - \frac{b}{3} \quad (\text{D12})$$

with $i = 1, 2, 3$.

Appendix E: Asymptotic zero-mass analysis of poles and relaxation time

From the definitions in Appendix D we obtain for the variables p, q appearing in Eq. (D12)

$$p = c - \frac{b^2}{3} = -\frac{\gamma/\tau + K}{m} + \frac{1}{3\tau^2}, \quad (\text{E1})$$

$$q = \frac{2b^3}{27} - \frac{cb}{3} + d = \frac{2i}{27\tau^3} + \frac{2iK}{3m\tau} - \frac{i\gamma}{3m\tau^2}. \quad (\text{E2})$$

We see that both p and q for small mass m diverge as m^{-1} , so the terms involving u_+ in Eq. (D12) are to leading orders in m (including the non-divergent m^0 contribution) given as

$$u_+ \simeq \frac{p^{1/2}}{\sqrt{3}} - \frac{q}{2p}, \quad (\text{E3})$$

$$\frac{p}{3u_+} \simeq \frac{p^{1/2}}{\sqrt{3}} + \frac{q}{2p}. \quad (\text{E4})$$

For the poles in Eq. (D12) we obtain to leading orders (including the m^0 contribution)

$$\omega_1 \simeq -\frac{q}{p} - \frac{b}{3} \simeq -\frac{iK}{mp\tau} \simeq \frac{iK}{\gamma + \tau K}, \quad (\text{E5})$$

$$\omega_2 \simeq ip^{1/2} + \frac{q}{2p} - \frac{b}{3}$$

$$\simeq -\left(\frac{K}{m}\right)^{1/2} \left(1 + \frac{\gamma}{\tau K}\right)^{1/2} + \frac{i\gamma/\tau^2}{2K(1 + \gamma/(\tau K))}, \quad (\text{E6})$$

$$\omega_3 \simeq -ip^{1/2} + \frac{q}{2p} - \frac{b}{3}$$

$$\simeq \left(\frac{K}{m}\right)^{1/2} \left(1 + \frac{\gamma}{\tau K}\right)^{1/2} + \frac{i\gamma/\tau^2}{2K(1 + \gamma/(\tau K))}. \quad (\text{E7})$$

We see that $\omega_1 \sim m^0$ while $\omega_2 \sim \omega_3 \sim m^{-1/2}$ for $m \rightarrow 0$. In particular, we obtain that that ω_2 and ω_3 have

a real part given by $(K/m)^{1/2}$ for large memory time τ , which is the oscillation frequency of the undamped Markovian harmonic oscillator, and an imaginary part given by $i\gamma/(2K\tau^2)$ for large memory time τ , which in the correlation function in Eqs. (65) leads to a long exponential decay time proportional to τ^2 , as indeed seen in Fig. 3(a). All sums and differences of two different poles diverge as $m^{-1/2}$ except

$$\omega_2 + \omega_3 \simeq q/p - 2b/3 \simeq \frac{i\gamma/\tau^2}{K(1 + \gamma/(\tau K))}. \quad (\text{E8})$$

This means that from the six terms contributing to τ_{rel} in Eq. (67) only the terms $I_1(\omega_1, \omega_2, \omega_3)$ and $I_2(\omega_1, \omega_2, \omega_3)$ defined in Eqs. (68) and (69) contribute. To leading order we obtain

$$\begin{aligned} I_1(\omega_1, \omega_2, \omega_3) &\equiv \frac{i(\tau - i/\omega_1)^2}{2\omega_1(\omega_1 - \omega_2)^2(\omega_1 - \omega_3)^2} \\ &\simeq \frac{i(\tau - i/\omega_1)^2}{2\omega_1\omega_2^2\omega_3^2} \simeq \frac{\gamma^2 m^2 \tau^2}{2K^3(\gamma + K\tau)}, \end{aligned} \quad (\text{E9})$$

$$\begin{aligned} I_2(\omega_1, \omega_2, \omega_3) &\equiv -\frac{2i(\tau - i/\omega_2)(\tau - i/\omega_3)}{(\omega_2 + \omega_3)(\omega_2 - \omega_1)(\omega_3 - \omega_1)(\omega_2 - \omega_3)^2} \\ &\simeq -\frac{2i\tau^2}{(\omega_2 + \omega_3)\omega_2\omega_3(\omega_2 - \omega_3)^2} \\ &\simeq \frac{m^2\tau^5}{2\gamma(\gamma + K\tau)}. \end{aligned} \quad (\text{E10})$$

Inserting these results into Eq. (67) we obtain

$$\begin{aligned} \tau_{\text{rel}} &\simeq \frac{2K^2}{m^2\tau^2} [I_1(\omega_1, \omega_2, \omega_3) + I_2(\omega_1, \omega_2, \omega_3)] \\ &\simeq \frac{2K^2}{m^2\tau^2} \left[\frac{\gamma^2 m^2 \tau^2}{2K^3(\gamma + K\tau)} + \frac{m^2\tau^5}{2\gamma(\gamma + K\tau)} \right] \\ &= \frac{\gamma^2}{K(\gamma + K\tau)} + \frac{K^2\tau^3}{\gamma(\gamma + K\tau)} \\ &= \frac{\gamma}{K} \left(\frac{1 + (\tau K/\gamma)^3}{1 + \tau K/\gamma} \right) \end{aligned} \quad (\text{E11})$$

which is Eq. (70).

Appendix F: Grote-Hynes Theory

The Grote-Hynes (GH) theory predicts the mean-first passage time to reach over the barrier, as illustrated in Fig. 1c), in the presence of memory friction as [54]

$$\tau_{\text{mfp}}^{\text{GH}} = \tau^{\text{TST}} \frac{\omega_{\text{max}}}{\lambda} = \frac{2\pi\omega_{\text{max}}}{\lambda\omega_{\text{min}}} e^{\beta U_0}, \quad (\text{F1})$$

where $\omega_{\text{max}} = \sqrt{K_{\text{bar}}/m}$ and $\omega_{\text{min}} = \sqrt{K/m}$ are the frequencies at the potential barrier and minimum (with

both curvatures defined as being positive) and τ^{TST} denotes the transition state theory prediction. λ is the barrier reactive frequency, which is determined by the GH equation

$$\lambda^2 + \lambda \frac{\hat{\Gamma}(\lambda)}{m} = \omega_{\max}^2, \quad (\text{F2})$$

where $\hat{\Gamma}(\lambda)$ is the Laplace transform of the friction memory kernel. For a single exponential memory kernel given by Eq. (53) we obtain

$$\hat{\Gamma}(\lambda) = \int_0^\infty \Gamma(t) e^{-\lambda t} dt = \frac{\gamma}{1 + \tau \lambda}. \quad (\text{F3})$$

Inserting (F3) into the GH equation (F2), we obtain a cubic polynomial. In the Markov limit $\tau \rightarrow 0$ we have $\hat{\Gamma}(\lambda) = \gamma$ and the solution of Eq. (F2) reads

$$\lambda = -\frac{\gamma}{2m} \pm \left(\frac{\gamma^2}{4m^2} + \omega_{\max}^2 \right)^{1/2}. \quad (\text{F4})$$

Taking the positive root, we obtain

$$\tau_{\text{mfp}}^{GH} = \omega_{\max} \left[\left(\frac{\gamma^2}{4m^2} + \omega_{\max}^2 \right)^{1/2} - \frac{\gamma}{2m} \right]^{-1} \tau^{TST}, \quad (\text{F5})$$

which is equivalent to the Kramers intermediate-to-high friction result. In the Markovian high-friction limit $\frac{\gamma}{m} \gg 1$ we obtain from Eq. (F5)

$$\tau_{\text{mfp}}^{GH} = \frac{2\pi\gamma}{K|K_{\text{bar}}|} e^{\beta U_0}, \quad (\text{F6})$$

which is identical to our result in Eq. (41) provided we choose for the relaxation time the result obtained in the Markovian mass-less limit $\tau_{\text{rel}} = \gamma/K$. In the Markovian low-friction limit $\frac{\gamma}{m} \ll 1$ we obtain from Eq. (F5)

$$\tau_{\text{mfp}}^{GH} = \tau^{TST}, \quad (\text{F7})$$

which means that in this limit GH theory becomes identical to transition state theory. As explained in Sec. II F 1 the transition state theory prediction corresponds to the prediction of the Kramers theory at the crossover between the high-friction and low-friction, the Kramers turnover, where the barrier crossing time has a minimum. Thus, the transition-state-theory prediction is a lower bound for the barrier-crossing time, friction and energy-diffusion effects increase the actual barrier-crossing time.

In the zero-mass $m \rightarrow 0$ limit the solution of the GH Eq. (F2) reads

$$\lambda = \frac{|K_{\text{bar}}|/\gamma}{1 - \tau|K_{\text{bar}}|/\gamma}, \quad (\text{F8})$$

so that we obtain

$$\tau_{\text{mfp}}^{GH} = \frac{2\pi\gamma(1 - \tau K_{\text{bar}}/\gamma)}{K} \left(\frac{K}{K_{\text{bar}}} \right)^{1/2} e^{\beta U_0}, \quad (\text{F9})$$

which agrees for small memory time τ exactly with our result in Eq. (71), except that the barrier curvature K_{bar} (which enters the GH theory) has to be replaced by K , the curvature at the potential bottom. So the GH theory correctly recovers the speed-up regime for small τ but misses the long-memory slow-down effect.

Appendix G: Derivation of time-reversal symmetry of the Mori GLE

In deriving a GLE, it is convenient (though not necessary) to consider a general time-independent Hamiltonian for a system of N interacting particles or atoms in three-dimensional space of the form

$$H(\omega) = \sum_{n=1}^N \frac{\mathbf{p}_n^2}{2m_n} + V(\{\mathbf{r}_N\}), \quad (\text{G1})$$

where a point in the $6N$ -dimensional phase space is denoted by $\omega = (\{\mathbf{r}_N\}, \{\mathbf{p}_N\})$, which is a $6N$ -dimensional vector consisting of the Cartesian particle positions $\{\mathbf{r}_N\}$ and the conjugate momenta $\{\mathbf{p}_N\}$ and fully specifies the microstate of the system. The Hamiltonian splits into a kinetic and a potential part and m_n is the mass of particle n . The potential $V(\{\mathbf{r}_N\})$ contains all interactions between the particles and includes possible external potentials. Using the Liouville operator

$$\mathcal{L}(\omega) = \sum_{n=1}^N \sum_{\alpha=x,y,z} \left(\frac{\partial H(\omega)}{\partial p_n^\alpha} \frac{\partial}{\partial r_n^\alpha} - \frac{\partial H(\omega)}{\partial r_n^\alpha} \frac{\partial}{\partial p_n^\alpha} \right), \quad (\text{G2})$$

the Heisenberg observable $B(w, t)$ is defined by propagation according to [70]

$$B(w, t) \equiv e^{(t-t_0)\mathcal{L}(w)} B_S(w), \quad (\text{G3})$$

where $B_S(w)$ is the ordinary time-independent observable, here denoted as Schrödinger observable in order to distinguish it from the Heisenberg observable. At time $t = t_0$ the Heisenberg observable coincides with the Schrödinger observable. In the following we assume that the observable $B_S(w)$ only depends on particle positions, i.e. $B_S(w) = B_S(\{\mathbf{r}\}_N)$. The time derivatives appearing in Eq. (75) follow from the propagator expression of $B(w, t)$ in Eq. (G3) as $\dot{B}(w, t) = \mathcal{L}(w)B(w, t)$ and $\ddot{B}(w, t) = \mathcal{L}^2(w)B(w, t)$. From the symmetry $H(\{\mathbf{r}_N\}, \{\mathbf{p}_N\}) = H(\{\mathbf{r}_N\}, -\{\mathbf{p}_N\})$ of the Hamiltonian Eq. (G1), the symmetry $\mathcal{L}(\{\mathbf{r}_N\}, \{\mathbf{p}_N\}) = -\mathcal{L}(\{\mathbf{r}_N\}, -\{\mathbf{p}_N\})$ of the Liouville operator Eq. (G2) and the propagator expression Eq. (G3), the time reversibility relations in Eq. (76) immediately follow.

The derivation of the GLE in Eq. (75) follows standard procedures [68]: One introduces a projection operator \mathcal{P} that acts on phase space functions and its complementary projection operator \mathcal{Q} via the relation $1 = \mathcal{Q} + \mathcal{P}$. Inserting this unit operator into the time propagator relation Eq. (G3), one obtains after a few steps the GLE in

Eq. (75), where t_P defines the time at which the projection is performed, which in principle can differ from the time t_0 at which the time propagation of the Heisenberg variable in Eq. (G3) starts [70].

The parameter K_M in Eq. (75) corresponds to the potential stiffness divided by the effective mass and is given by

$$K_M = \frac{\langle (\mathcal{L}B(\omega, t_P))^2 \rangle}{\langle (B(\omega, t_P) - \langle B \rangle)^2 \rangle}. \quad (\text{G4})$$

Here we define the expectation value of an arbitrary phase-space function $X(\omega)$ with respect to a time-independent projection distribution $\rho_P(\omega)$ as

$$\langle X(\omega) \rangle = \int d\omega X(\omega) \rho_P(\omega), \quad (\text{G5})$$

which we here take to be the normalized equilibrium canonical distribution $\rho_P(\omega) = e^{-H(\omega)/(k_B T)}/Z$, where Z is the canonical partition function $Z = \int d\omega e^{-H(\omega)/(k_B T)}$. Obviously, the parameter K_M is independent of time and particle momenta and therefore not influenced by momentum or time reversal.

The complementary force in Eq. (75) is given by

$$F_M(\omega, t) \equiv e^{(t-t_P)\mathcal{Q}\mathcal{L}} \mathcal{Q}\mathcal{L}^2 B(\omega, t_P) \quad (\text{G6})$$

and the memory friction kernel is given by [70]

$$\Gamma_M(t) = \frac{\langle F_M(\omega, 0) F_M(\omega, t) \rangle}{\langle (\mathcal{L}B(\omega, t_P))^2 \rangle}. \quad (\text{G7})$$

From the fact that the Liouville operator is anti-self-adjoint and that the complementary projection operator \mathcal{Q} is self-adjoint and idempotent, i.e. $\mathcal{Q}^2 = \mathcal{Q}$, it follows that the memory friction kernel is a symmetric function, i.e. $\Gamma_M(t) = \Gamma_M(-t)$, which is used to derive the time reversibility of the friction-memory term in Eq. (77).

[1] H. A. Kramers, Brownian motion in a field of force and the diffusion model of chemical reactions, *Physica* **7**, 284 (1940).

[2] P. B. Visscher, Escape rate for a Brownian particle in a potential Well, *Phys. Rev. B* **13**, 3272 (1976).

[3] D. Chandler, Statistical mechanics of isomerization dynamics in liquids and the transition state approximation, *J. Chem. Phys.* **68**, 2959 (1978).

[4] J. L. Skinner and P. G. Wolynes, Relaxation processes and chemical kinetics, *J. Chem. Phys.* **69**, 2143 (1978).

[5] J. T. Hynes, Chemical Reaction Dynamics in Solution, *Ann. Rev. Phys. Chem.* **36**, 573 (1985).

[6] B. J. Berne, M. Borkovec, and J. E. Straub, Classical and modern methods in reaction rate theory, *The Journal of Physical Chemistry* **92**, 3711 (1988).

[7] P. Hänggi, P. Talkner, and M. Borkovec, Reaction-rate theory: fifty years after Kramers, *Reviews of Modern Physics* **62**, 251 (1990).

[8] S. Arrhenius, Über die Reaktionsgeschwindigkeit bei der Inversion von Rohrzucker durch Säuren, *Zeitschrift für Physikalische Chemie* **4U**, 226 (1889).

[9] H. Eyring, The Activated Complex in Chemical Reactions, *The Journal of Chemical Physics* **3**, 107 (1935).

[10] K. J. Laidler and M. C. King, Development of transition-state theory, *The Journal of Physical Chemistry* **87**, 2657 (1983).

[11] M. P. Allen, Brownian dynamics simulation of a chemical reaction in solution, *Mol. Phys.* **40**, 1073 (1980).

[12] J. Trullàs, A. Giró, and J. A. Padró, Langevin dynamics study of NaCl electrolyte solutions at different concentrations, *J. Chem. Phys.* **93**, 5177 (1990).

[13] B. Lickert and G. Stock, Modeling non-Markovian data using Markov state and Langevin models, *J. Chem. Phys.* **153**, 244112 (2020).

[14] V. I. Mel'nikov and S. V. Meshkov, Theory of activated rate processes: Exact solution of the Kramers problem, *The Journal of Chemical Physics* **85**, 1018 (1986).

[15] H. Grabsht, Escape from a Metastable Well: The Kramers Turnover Problem, *Phys. Rev. Lett.* **61**, 1988 (1988).

[16] R. B. Best and G. Hummer, Diffusive model of protein folding dynamics with Kramers turnover in rate., *Physical Review Letters* **96**, 228104 (2006).

[17] R. Zwanzig, Memory Effects in Irreversible Thermodynamics, *Physical Review* **124**, 983 (1961).

[18] H. Mori, Transport, Collective Motion, and Brownian Motion, *Progress of Theoretical Physics* **33**, 423 (1965).

[19] S. Acharya and B. Bagchi, Non-Markovian rate theory on a multidimensional reaction surface: Complex interplay between enhanced configuration space and memory, *J. Chem. Phys.* **156**, 134101 (2022).

[20] J. E. Straub, M. Borkovec, and B. J. Berne, Calculation of dynamic friction on intramolecular degrees of freedom, *The Journal of Physical Chemistry* **91**, 4995 (1987).

[21] C. Hijón, P. Español, E. Vanden-Eijnden, and R. Delgado-Buscalioni, Mori-Zwanzig formalism as a practical computational tool, *Faraday Discussions* **144**, 301 (2010).

[22] A. Carof, R. Vuilleumier, and B. Rotenberg, Two algorithms to compute projected correlation functions in molecular dynamics simulations, *The Journal of Chemical Physics* **140**, 124103 (2014), publisher: American Institute of Physics.

[23] G. Jung, M. Hanke, and F. Schmid, Iterative Reconstruction of Memory Kernels, *Journal of Chemical Theory and Computation* **13**, 2481 (2017).

[24] J. O. Daldrop, B. G. Kowalik, and R. R. Netz, External Potential Modifies Friction of Molecular Solutes in Water, *Physical Review X* **7**, 041065 (2017).

[25] J. O. Daldrop, J. Kappler, F. N. Brünig, and R. R. Netz, Butane dihedral angle dynamics in water is dominated by internal friction, *Proceedings of the National Academy of Sciences* **115**, 5169 (2018).

[26] B. Kowalik, J. O. Daldrop, J. Kappler, J. C. F. Schulz,

A. Schlaich, and R. R. Netz, Memory-kernel extraction for different molecular solutes in solvents of varying viscosity in confinement, *Physical Review E* **100**, 012126 (2019).

[27] F. Grogan, H. Lei, X. Li, and N. A. Baker, Data-Driven Molecular Modeling with the Generalized Langevin Equation, *Journal of Computational Physics* **418**, 109633 (2020).

[28] V. Klippenstein, M. Tripathy, G. Jung, F. Schmid, and N. F. A. van der Vegt, Introducing Memory in Coarse-Grained Molecular Simulations, *The Journal of Physical Chemistry B* **125**, 4931 (2021).

[29] H. Vroylandt, L. Goudenège, P. Monmarché, F. Pietrucci, and B. Rotenberg, Likelihood-based non-markovian models from molecular dynamics, *Proceedings of the National Academy of Sciences* **119**, e2117586119 (2022).

[30] L. Tepper, B. A. Dalton, and R. R. Netz, Accurate Memory Kernel Extraction from Discretized Time-Series Data, *Journal of Chemical Theory and Computation* **20**, 3061 (2024).

[31] M. Tuckerman and B. Berne, Vibrational relaxation in simple fluids: Comparison of theory and simulation, *The Journal of Chemical Physics* **98**, 7301 (1993).

[32] F. Gottwald, S. D. Ivanov, and O. Kühn, Applicability of the Caldeira–Leggett model to vibrational spectroscopy in solution, *The Journal of Physical Chemistry Letters* **6**, 2722 (2015).

[33] F. N. Brünig, O. Geburtig, A. von Canal, J. Kappler, and R. R. Netz, Time-Dependent Friction Effects on Vibrational Infrared Frequencies and Line Shapes of Liquid Water, *The Journal of Physical Chemistry B* **126**, 1579 (2022).

[34] B. Bagchi and D. W. Oxtoby, The effect of frequency dependent friction on isomerization dynamics in solution, *The Journal of Chemical Physics* **78**, 2735 (1983).

[35] B. A. Dalton, H. Kiefer, and R. R. Netz, The Role of Memory-Dependent Friction and Solvent Viscosity in Isomerization Kinetics in Viscogenic Media, *Nature Communications* **15**, 3761 (2024).

[36] S. A. Adelman, Generalized Langevin theory for many-body problems in chemical dynamics: Reactions in liquids, *J. Chem. Phys.* **73**, 3145 (1980).

[37] G. Ciccotti and J.-P. Ryckaert, On the derivation of the generalized Langevin equation for interacting Brownian particles, *Journal of Statistical Physics* **26**, 73 (1981).

[38] S. Wolf, B. Lickert, S. Bray, and G. Stock, Multisecond ligand dissociation dynamics from atomistic simulations, *Nat. Commun.* **11**, 2918 (2020).

[39] F. N. Brünig, J. O. Daldrop, and R. R. Netz, Pair-Reaction Dynamics in Water: Competition of Memory, Potential Shape, and Inertial Effects, *The Journal of Physical Chemistry B* **126**, 10295 (2022).

[40] S. S. Plotkin and P. G. Wolynes, Non-Markovian Configurational Diffusion and Reaction Coordinates for Protein Folding, *Physical Review Letters* **80**, 5015 (1998).

[41] O. F. Lange and H. Grubmüller, Collective Langevin dynamics of conformational motions in proteins, *The Journal of Chemical Physics* **124**, 214903 (2006).

[42] R. Satija and D. E. Makarov, Generalized Langevin Equation as a Model for Barrier Crossing Dynamics in Biomolecular Folding, *The Journal of Physical Chemistry B* **123**, 802 (2019).

[43] H. S. Lee, S.-H. Ahn, and E. F. Darve, The multi-dimensional generalized langevin equation for conformational motion of proteins, *The Journal of chemical physics* **150**, 174113 (2019).

[44] C. Ayaz, L. Tepper, F. N. Brünig, J. Kappler, J. O. Daldrop, and R. R. Netz, Non-Markovian modeling of protein folding, *Proceedings of the National Academy of Sciences* **118**, 10.1073/pnas.2023856118 (2021).

[45] B. A. Dalton, C. Ayaz, H. Kiefer, A. Klimek, L. Tepper, and R. R. Netz, Fast protein folding is governed by memory-dependent friction, *Proceedings of the National Academy of Sciences* **120**, e2220068120 (2023).

[46] D. T. Schmitt and M. Schulz, Analyzing Memory Effects of Complex Systems from Time Series, *Physical Review E* **73**, 056204 (2006).

[47] B. G. Mitterwallner, C. Schreiber, J. O. Daldrop, J. O. Rädler, and R. R. Netz, Non-Markovian data-driven modeling of single-cell motility, *Physical Review E* **101**, 032408 (2020).

[48] E. Herrera-Delgado, J. Briscoe, and P. Sollich, Tractable nonlinear memory functions as a tool to capture and explain dynamical behaviors, *Physical Review Research* **2**, 043069 (2020).

[49] F. Hassanibesheli, N. Boers, and J. Kurths, Reconstructing Complex System Dynamics from Time Series: A Method Comparison, *New Journal of Physics* **22**, 073053 (2020).

[50] O. Vilk, R. Metzler, and M. Assaf, Non-markovian gene expression, *Phys. Rev. Res.* **6**, L022026 (2024).

[51] A. Klimek, D. Mondal, S. Block, P. Sharma, and R. R. Netz, Data-driven classification of individual cells by their non-Markovian motion, *Biophysical Journal* **123**, 1 (2024).

[52] H. Kiefer, D. Furtel, C. Ayaz, A. Klimek, J. O. Daldrop, and R. R. Netz, Prediction of weather and financial time-series data via a Hamiltonian-based filter-projection approach, *Newton* **1**, 100138 (2025).

[53] B. A. Dalton, A. Klimek, H. Kiefer, F. N. Brünig, H. Colinet, L. Tepper, A. Abbasi, and R. R. Netz, Memory and Friction: From the Nanoscale to the Macroscale, *Annu. Rev. Phys. Chem.* **76**, 431 (2025).

[54] R. F. Grote and J. T. Hynes, The stable states picture of chemical reactions. II. Rate constants for condensed and gas phase reaction models, *The Journal of Chemical Physics* **73**, 2715 (1980).

[55] R. Biswas and B. Bagchi, Activated barrier crossing dynamics in slow, viscous liquids, *J. Chem. Phys.* **105**, 7543 (1996).

[56] D. G. Truhlar and B. C. Garrett, Multidimensional Transition State Theory and the Validity of Grote-Hynes Theory, *J. Phys. Chem. B* **104**, 1069 (2000).

[57] E. Pollak, H. Grabert, and P. Hänggi, Theory of activated rate processes for arbitrary frequency dependent friction: Solution of the turnover problem, *The Journal of Chemical Physics* **91**, 4073 (1989).

[58] E. Pollak and P. Talkner, Activated rate processes: Finite-barrier expansion for the rate in the spatial-diffusion limit, *Physical Review E* **47**, 922 (1993).

[59] J. D. Bryngelson, J. N. Onuchic, N. D. Socci, and P. G. Wolynes, Funnels, pathways, and the energy landscape of protein folding: A synthesis, *Proteins: Structure* **21** (1995).

[60] A. Berezhkovskii and A. Szabo, One-dimensional reaction coordinates for diffusive activated rate processes in many dimensions, *The Journal of Chemical Physics* **122**,

14503 (2004).

[61] O. K. Dudko, G. Hummer, and A. Szabo, Intrinsic Rates and Activation Free Energies from Single-Molecule Pulling Experiments, *Physical Review Letters* **96**, 108101 (2006).

[62] B. Schüller, A. Meistrenko, H. van Hees, Z. Xu, and C. Greiner, Kramers' escape rate problem within a non-Markovian description, *Annals of Physics* **412**, 168045 (2020).

[63] J. E. Straub, M. Borkovec, and B. J. Berne, Non-Markovian activated rate processes: Comparison of current theories with numerical simulation data, *The Journal of Chemical Physics* **84**, 1788 (1986).

[64] J. Kappler, J. O. Daldrop, F. N. Brünig, M. D. Boehle, and R. R. Netz, Memory-induced acceleration and slowdown of barrier crossing, *The Journal of Chemical Physics* **148**, 14903 (2018).

[65] J. Kappler, V. B. Hinrichsen, and R. R. Netz, Non-Markovian barrier crossing with two-time-scale memory is dominated by the faster memory component, *The European Physical Journal E* **42**, 119 (2019).

[66] L. Lavacchi, J. Kappler, and R. R. Netz, Barrier crossing in the presence of multi-exponential memory functions with unequal friction amplitudes and memory times, *Europhysics Letters* **131** (2020).

[67] R. R. Netz, Time-dependent trajectory of a one-dimensional gaussian non-markovian observable does not reveal its nonequilibrium character, *Phys. Rev. E* **112**, 014132 (2025).

[68] R. Zwanzig, *Nonequilibrium statistical mechanics* (Oxford UnivPress, Oxford [u.a.], 2001).

[69] E. S. E. S. Nascimento and W. A. M. Morgado, Non-Markovian effects on overdamped systems, *Europhys. Lett.* **126**, 10002 (2019).

[70] R. R. Netz, Temporal coarse graining and elimination of slow and periodic dynamics with the generalized langevin equation for convolution-time-filtered observables, *Phys. Rev. E* **111**, 054132 (2025).

[71] L. Lavacchi, B. A. Dalton, and R. R. Netz, Non-Markovian equilibrium and non-equilibrium barrier-crossing kinetics in asymmetric double-well potentials, *The European Physical Journal E* **48**, 26 (2025).

[72] Q. Zhou, A. Bakaev, L. Lavacchi, R. R. Netz, and B. A. Dalton, Rapid state-recrossing kinetics and slow escape kinetics in non-Markovian systems, *Physical Review* **111**, 064110 (2025).